Epigenetic control of alveolar fluid clearance

Inauguraldissertation
zur Erlangung des Grades eines Doktors der Humanbiologie
des Fachbereichs Medizin
der Justus-Liebig-Universität Gießen

vorgelegt von Łukasz Andrzej Wujak
aus Thorn, Polen

Giessen, 2014

Aus dem
Max-Planck-Institut für Herz- und Lungenforschung, Bad Nauheim
Leiter/Direktor: Prof. Dr. Werner Seeger

Gutachter: Prof. Dr. med. Markus Weigand

Tag der Disputation: 12. Juni 2014

I. Table of contents

II. List of figures

III. List of tables

IV. List of abbreviations

AETI	alveolar epithelial type I
AETII	alveolar epithelial type II
AFC	alveolar fluid clearance
ALK	activin receptor-like kinase
ANF	atrial natriuretic factor
APACHE	acute physiology and chronic health evaluation
APS	ammonium persulfate
ARDS	acute respiratory distress syndrome
ATF	activating transcription factor
ATP	adenosine triphosphate
5-Aza-2′-dC	5-Aza-2′deoxycytidine
BAL	broncho-alveolar lavage
bp	base pair(s)
bZIP	basic leucine zipper
cAMP	cyclic adenosine monophosphate
CBP	CREB binding protein
ChIP	chromatin immunoprecipitation
CFTR	cystic fibrosis transmembrane conductance regulator
COL1A2	alpha-2 type I collagen
CtBP	C-terminal binding protein
DNA-BP	DNA-binding protein
DMEM	Dulbecco’s modified Eagle’s medium
DSP	3,3′-Dithiodipropionic acid di(N-hydroxysuccinimide ester)
DTT	dithiothreitol
EDTA	ethylene dinitril *o*-N,N,*N*′,*N*′-tetraacetic acid
EGF	epidermal growth factor
EGTA	ethylene glycol-bis (2-aminoethylether)-
	-N,N,*N*′,*N*′-tetraacetic acid
ENaC	epithelial sodium channel
EVI-1	ecotropic virus integration site 1 protein homolog
FCS	fetal calf serum

FiO_2	fraction of inspired oxygen
FoxO	forkhead box protein O
g	gram(s)
h	hour(s)
HAT	histone acetyltransferases
HDAC	histone deacetylase
kg	kilogram(s)
KGF	keratinocyte growth factor
LB-medium	Luria-Bertani medium
MAD	mothers against decapentaplegic
mg	milligram(s)
MH	Mad homolgy
min	minute(s)
ml	milliliter(s)
mM	millimolar
mmHg	millimeter mercury
mV	millivolt(s)
Na,K-ATPase	sodium/potassium-exchanging ATPase
N-CoR	nuclear receptor co-repressor 1
ng	nanogram(s)
nM	nanomolar
nm	nanometer(s)
PaO_2	partial pressure of oxygen in arterial blood
PBS	phosphate buffered saline
PCAF	p300/CBP-associated factor
PCR	polymerase chain reaction
Pol II	RNA polymerase II
qPCR	quantitative PCR
rpm	revolutions per minute
R-SMAD	receptor SMAD
RT	room temperature
RUNX2	Runt-related transcription factor 2
s	second(s)

SDS	sodium dodecyl sulfate
SEM	standard error of the mean
SKI	Sloan-Kettering institute
SnoN	Ski-related novel protein N
Sp1	specificity protein 1
SWI/SNF	switch/sucrose nonfermentable
TBRI	TGF-β receptor type I
TBRII	TGF-β receptor type II
TEMED	N,N,*N´*,*N´*-tetramethylethane-1,2-diamine
TFE3	transcription factor E3
TFIID	transcription factor II D
TGF-α	transforming growth factor-α
TGF-β	transforming growth factor-β
TGFBR2	TGF-β receptor type 2
TGIF	transforming growth interacting factor
TSA	trichostatin A
µg	microgram(s)
µl	microliter(s)
µM	micromolar
µm	micrometer(s)
YY1	yin-yang 1

1. Introduction

1.1. Acute respiratory distress syndrome

Acute respiratory distress syndrome (ARDS) is a clinical syndrome which develops rapidly and results in respiratory failure. A recently proposed interpretation of ARDS, the Berlin definition, includes a value of the PaO_2/FiO_2 ratio of below 300 mmHg, acute onset and the presence of bilateral opacities present on chest radiographs consistent with pulmonary edema (Ranieri *et al*., 2012). The disease is categorized by the degree of hypoxemia: mild (PaO_2/FiO_2 ratio between 300 and 200 mmHg), moderate (PaO_2/FiO_2 ratio between 200 and 100 mmHg) or severe (PaO_2/FiO_2 ratio below 100 mmHg). Patients with ARDS require urgent admission to critical care units for advanced life support and utilize considerable health care resources.

Acute respiratory distress syndrome has multiple etiologies and can develop as a result of direct injury to the lungs, such as after viral or bacterial pneumonia, aspiration of gastric contents, or smoke or toxic gas inhalation. Alternatively, ARDS can occur indirectly during the course of systemic inflammation, such as during sepsis; or after trauma or blood transfusion (Ware and Matthay, 2000). The risk of ARDS development is higher in patients with pneumonia, severe sepsis, and aspiration of gastric contents, hemorrhage or trauma (Matthay and Zemans, 2011). Multi-organ failure is the most common cause of death in patients with ARDS (Lipes *et al.*, 2012). The mortality rate of ARDS is 27-45% and depends on the severity of disease (Ranieri *et al*., 2012). Mortality risk depends on the nature of the underlying disorder and is higher for patients with sepsis, pneumonia or aspiration (Rubenfeld *et al*., 2005; Eisner *et al*., 2001). Additionally, the risk of death is influenced by age and race, since younger patients have lower mortality rates and Afro-Americans or Hispanics have increased risk of death when compared to Caucasians (Rubenfeld *et al*., 2005; Eisner *et al.*, 2001). Currently, the therapy for ARDS remains limited to lung-protective mechanical ventilation while several pharmacological therapies evaluated have proven to be ineffective.

1.1.1. Pathology of acute respiratory distress syndrome

The alveolar-capillary barrier is the basic functional unit of the lung, formed by adjacent layers of the alveolar epithelium, a basement membrane and the microvascular endothelium. The integrity of this delicate system is crucial for maintaining liquid homeostasis in the lung, leaving the alveolar surface relatively dry and, ultimately, allowing effective gas exchange.

Irrespective of the nature of the primary insult triggering ARDS, specific histopathological characteristics are common to all ARDS pathology. Based on histological evidence, the progression of ARDS can be divided into three phases, with the acute phase being the most immediate, followed first by the proliferative and then the fibrotic stages, which together constitute the chronic phase.

The acute phase persists during the initial seven days after insult to the lung. In the acute phase, the alveolar-capillary barrier is destroyed, which causes permeability and alveolar flooding. In consequence, pulmonary edema develops, which decreases the efficiency of gas exchange, and eventually causes respiratory failure. Cell necrosis, inflammation and fibrotic processes, collectively referred to as diffuse alveolar damage, are routinely observed and are responsible for loss of alveolar-capillary barrier integrity (Ware and Matthay, 2000). The key histopathological features of the acute phase of ARDS are demonstrated in Figure 1.

The majority of patients who survive the acute stage of ARDS enter the proliferative phase, which is characterized by the presence of hyperplastic alveolar epithelial type II (AETII) cells and fibroblasts. The AETII cells migrate along alveolar septa and proliferate in order to reconstitute epithelial integrity (Geiser, 2003). Additionally, fibroblasts deposit extracellular matrix proteins which transform the intra-alveolar space into fibrous tissue and obliterate the alveolar space (Marshall *et al.*, 1998).

The effort of epithelial repair undertaken during the proliferative phase may result in complete restoration of lung function. Nevertheless, proper re-epithelialization is frequently disturbed and can cause progression into the fibrotic phase of ARDS (Ware and Matthay, 2000). In this final stage, the alveolar space is filled with proliferating fibroblasts, abnormal amounts of extracellular matrix and new blood vessels, a characteristic collectively described as fibrosing alveolitis (Ware, 2006).

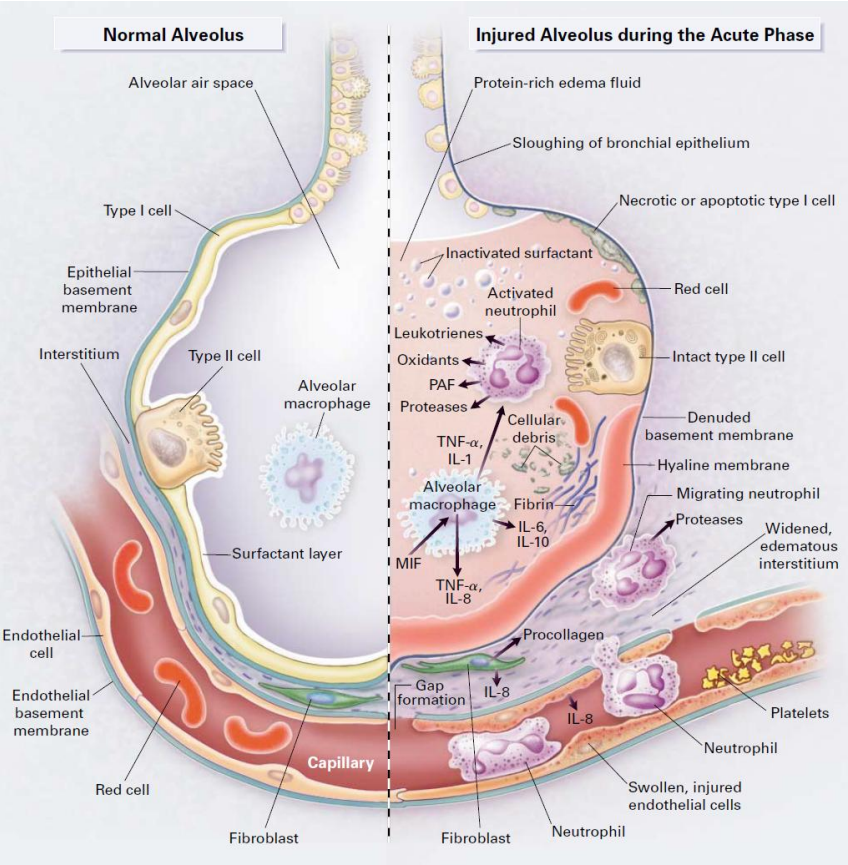

Figure 1. Comparison of a healthy alveolus to a damaged alveolus in the acute phase of acute respiratory distress syndrome. A healthy alveolus (left-hand side) is characterized by the presence of intact endothelial and epithelial barriers and balanced regulation of the alveolar fluid volume and composition. In the acute respiratory distress syndrome (right-hand side), the integrity of the alveolar-capillary barrier is lost, which promotes accumulation of protein-rich edema fluid in the alveoli (from Ware and Matthay, 2000).

1.1.2. Injury to the alveolar-capillary barrier promotes edema formation and persistence in acute respiratory distress syndrome

Damage to the endothelial and epithelial barriers perturbs fluid balance and leads to alveolar flooding in the acute phase of ARDS (Ware, 2006). The injury to the pulmonary vasculature was documented by Tomashefski *et al.*, who reported substantial ultrastructural lesions in the capillary endothelium in patients with ARDS (Tomashefski *et al.*, 1983). It appears that granulocyte recruitment in the pulmonary microvasculature is responsible for capillary endothelial damage (Looney *et al.*, 2006). Activated,

degranulating neutrophils are a source of proteases, proinflammatory cytokines, procoagulants and reactive oxygen species, all of which can injure microvascular endothelial cells and cause extravasation of protein-rich fluid (Matthay and Zemans, 2011). However, despite that endothelial dysfunction is evident in ARDS, increased vascular permeability is insufficient to facilitate edema formation in presence of a morphologically and functionally intact alveolar epithelium, suggesting that injury to the endothelium alone is incapable to cause ARDS (Wiener-Kronish *et al.*, 1991).

The intensity of the injury to the epithelium and edema level correlates with the severity of the ARDS and is associated with poor outcome (Ware and Matthay, 2001, Matthay and Wiener-Kronish, 1990). Destruction of the epithelial wall results in functional impairment of lung function on multiple levels. Since alveolar epithelial cells are exceptionally tightly connected, the epithelial barrier is much less permeable compared to the microvascular endothelial barrier. Therefore, loss of epithelial wall integrity has more severe consequences than the destruction of the endothelial layer, and contributes to the accumulation of protein-rich edema fluid in the alveoli to a high degree (Wiener-Kronish *et al.*, 1991). An ultrastructural study of epithelial injury in ARDS revealed cell vacuolization, cytoplasmic swelling, focal detachment from the basement membrane, and necrosis (Ware, 2006, Tomashefski, 2000). Eradication of alveolar epithelial type I (AETI) cells results in a reduction of gas exchange surface area and delivers a major initial blow to epithelial layer integrity, allowing the influx of edema fluid into the alveolar space (Ware and Matthay, 2000). On the contrary, AETII cells seem to be more resistant to the initial insult. Additionally, AETII cells proliferate and differentiate into AETI cells and are critical for re-epithelization and repair of the alveolar epithelium after injury (Geiser, 2003).

Apart from increased fluid permeability, the destruction of the epithelial layer has another fundamental consequence in the form of perturbed lung liquid reabsorption in ARDS (Modelska *et al.*, 1999, Laffon *et al.*, 1999). The major force driving water movement in the lung is Na^+ transport from the alveolar lumen across the epithelium *via* the apically-located epithelial sodium channel (ENaC) and the basolaterally-located sodium/potassium-exchanging ATPase (Na,K-ATPase) into the interstitium (Matthay *et al.*, 2002). The polarized distribution of Na^+ transporters in the plasma membranes of alveolar epithelial cells is essential for vectorial Na^+ transport and formation of an osmotic gradient, which is followed by isoosmotic water reabsorption from the alveoli in the process of alveolar fluid clearance (AFC) (Matthay *et al.*, 2002).

1.2. Alveolar fluid clearance

Both AETI and AETII cells express elements of the Na^+ transporting machinery and are able to perform Na^+ ion transport and drive AFC (Matthay and Zimmerman, 2005). The function of ENaC is to passively conduct Na^+ ions from alveolar space into alveolar epithelial cells (Guidot *et al.*, 2006). Four types of subunits, α-ENaC, β-ENaC, γ-ENaC and δ-ENaC were found in human lung epithelial cells (Zhao *et al.*, 2012, Berthiaume and Matthay, 2007). The role of ENaC is important for lung fluid homeostasis, since inhibition of ENaC by amiloride partially prevents Na^+ uptake by AETI cells *in vitro* and inhibits basal AFC in human and other mammalian lungs (Matthay *et al.*, 2002). Furthermore, deletion or diminished expression of the mouse α-ENaC gene results in pulmonary edema and causes respiratory distress syndrome (Egli *et al.*, 2004, Matthay *et al.*, 2002). The activity of ENaC can be directly modulated by cAMP, or indirectly, *via* regulation of gene expression, by glucocorticoids and catecholamines (Berthiaume and Matthay, 2007). Additionally, the cystic fibrosis transmembrane conductance regulator (CFTR), a Cl^- ion channel expressed in AETI and AETII cells, has been also found to be involved in the AFC process (Berthiaume and Matthay, 2007).

The Na,K-ATPase generates an electrochemical gradient across the basolateral membrane of AETI and AETII cells by actively pumping K^+ ions into the cell, and extruding Na^+ ions into the interstitium. An analysis of the Na,K-ATPase pump structure revealed the presence of three types of subunits: ATP1A, ATP1B and FXYD (also known as α, β and γ proteins, respectively). The structure of Na,K-ATPase is illustrated in Figure 2. The ATP1A and ATP1B subunits form the core of the Na,K-ATPase, and are indispensable for pump function (Geering, 2008). The ATP1A subunit, which has four isoforms (ATP1A1-ATP1A4), is the catalytic unit that transports Na^+ and K^+ ions and hydrolyzes ATP, which is required for ion-conducting activity. Since ATP1A is unable to localize itself into cell membrane, the presence of the ATP1B subunit (isoforms ATP1B1-ATP1B3) is critically required for assembly, membrane insertion and stability of the Na,K-ATPase complex, and only the ATP1A-ATP1B heterodimer can perform pump function (Geering, 2006). Moreover, Barquin and colleagues have suggested that ATP1B1 subunit abundance is the rate limiting factor for Na,K-ATPase assembly and activity in isolated rat AETII cells and the lung (Barquin *et al.*, 1997).

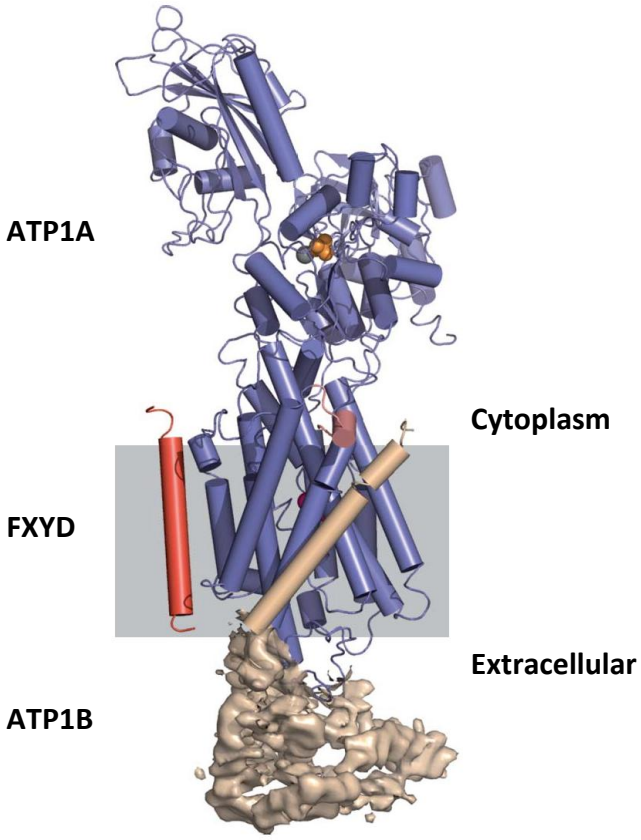

Figure 2. Architecture of the Na,K-ATPase. The X-ray crystal structure at 3.5 Å resolution of the porcine renal Na,K-ATPase consisting of ATP1A (blue), ATP1B (brown) and FXYD (red) subunits (adapted from Morth *et al*., 2007).

The activity of the Na,K-ATPase is carefully controlled, and involves direct and indirect mechanisms. Direct mechanisms include covalent modifications and allosteric structure fine-tuning. The indirect system of regulation includes trafficking of the Na,K-ATPase between plasma membrane and endosomal pools, and synthesis/degradation rate adjustment (Matthay *et al.*, 2002). Moreover, modulation of the expression of Na,K-ATPase-encoding genes by hyperoxia or β-adrenergic, glucocorticoid/mineralocorticoid and thyroid systems has also been reported (Berthiaume and Matthay, 2007, Matthay *et al.*, 2002). Complex regulation of pump-encoding gene transcription and mRNA translation have a persistent effect on Na,K-ATPase activity, while dopaminergic and adrenergic stimulation rapidly induce Na,K-ATPase phosphorylation and trafficking to the cell membrane (Matthay *et al.*, 2002). Finally, studies with the Na,K-ATPase inhibitor ouabain in AETII cells, in

resected human lungs and in live animals revealed that the Na,K-ATPase is essential for Na^+ transport and AFC in intact healthy lungs as well as after injury (Berthiaume and Matthay, 2007, Matthay *et al.*, 2002).

1.2.1. Alveolar fluid clearance is impaired in acute respiratory distress syndrome

A damaged and permeable alveolar epithelium allows rapid water accumulation and edema formation which cannot be resolved because of impaired AFC processes caused by defective ion transport (Sartori and Matthay, 2002). A number of factors have been shown to perturb transepithelial ion transport and, consequently, decrease AFC (highlighted in Figure 3). After lung injury, Na^+ transport *via* ENaC and the Na,K-ATPase can be directly reduced by secondary inflammatory mediators including reactive oxygen and nitrogen species (Lecuona *et al.*, 2007, Morty *et al*., 2007, Matthay *et al*., 2002). Hypoxia, which develops during ARDS, reduces Na^+ transport in AETII cells and impairs the AFC process (Sartori and Matthay, 2002). Various cytokines that are involved in the pathogenesis of ARDS, including tumor necrosis factor-α, interleukin-1β and transforming growth factor (TGF)-β, and infectious agents, including *Pseudomonas* or influenza virus; inhibit Na^+ transport and prevent AFC (Morty *et al*., 2007, Frank *et al.*, 2003, Matthay *et al*., 2002, Evans *et al.*, 1998). Additionally, active Na^+ transport and subsequent AFC are inhibited by Na,K-ATPase endocytosis early in sepsis-induced lung injury (Berger *et al.*, 2011). Lecuona and colleagues described a reduction in Na,K-ATPase function in AETII cells in a rat model of ventilator-induced ARDS. Since AFC in these animals was also reduced, this study highlights the importance of proper patient ventilation in the intensive care unit, which must not further hamper already weakened Na^+ transport and edema fluid resolution mechanisms (Lecuona *et al.*, 1999). Despite the strong evidence for decreased transepithelial Na^+ transport in various models of ARDS, it is important to note that mild lung injury can have the opposite effect and improve Na^+ transport and AFC (Matthay *et al*., 2002). Increased Na^+ uptake after mild lung injury may serve as a natural mechanism preventing alveolar flooding and may offer some protection against lung injury.

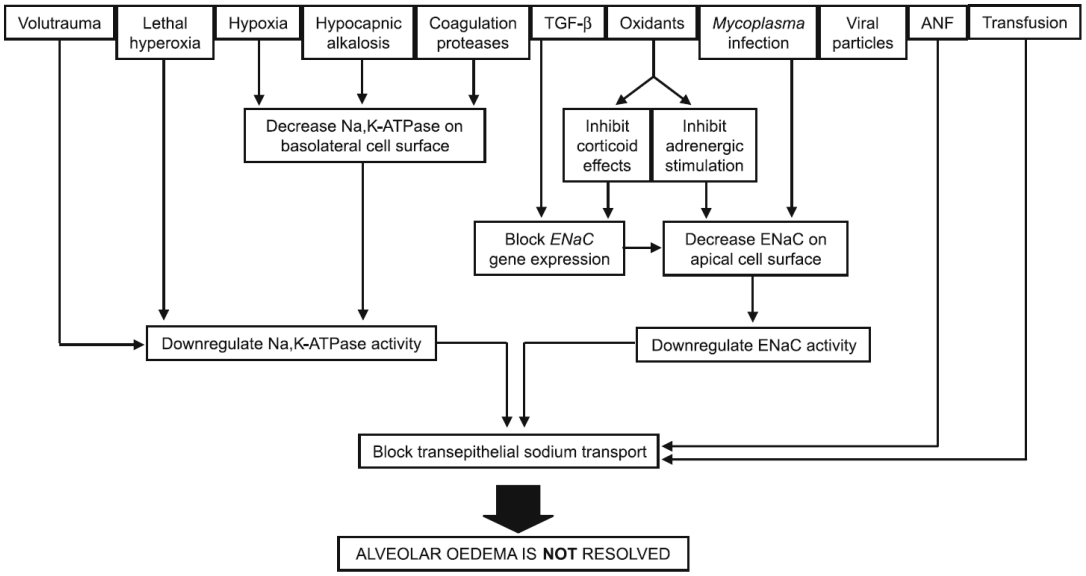

Figure 3. Mechanisms of perturbed alveolar fluid clearance leading to the formation and persistence of pulmonary edema after lung injury. TGF-β, transforming growth factor-β; ANF, atrial natriuretic factor (from Morty *et al*., 2007).

1.2.2. Upregulation of alveolar fluid clearance can improve acute respiratory distress syndrome

Several clinical studies demonstrate that patients with enhanced AFC display improvement in ARDS and increased survival in contrast to those without efficient AFC function (Ware and Matthay, 2001, Matthay and Wiener-Kronish, 1990, Ware *et al.*, 1999). Therefore, it is reasonable to preserve and, if possible, to increase AFC in the lungs of ARDS patients (Berthiaume and Matthay, 2007, Sartori and Matthay, 2002). A number of experimental studies have demonstrated the positive impact of Na^+ transport reactivation on increased AFC in animal models of ARDS (reviewed by Morty *et al*., 2007 and Sartori and Matthay, 2002; summarized in Figure 4). Dopamine and β_2-agonists have been reported to stimulate AFC in multiple experimental models of ARDS by exocytosis of Na,K-ATPase from intracellular pools to the basolateral cell membrane of alveolar epithelial cells. The positive effect of β_2-agonists on pulmonary edema resolution in humans has been reported by Perkins and colleagues, who observed decreased lung water in a randomized placebo-controlled clinical phase II trial of 40 ARDS patients receiving intravenous salbutamol (Perkins *et al.*, 2006). However, despite these encouraging results, large, randomized and placebo-controlled clinical trial

on 282 patients with ARDS did not demonstrate increased number of ventilator-free days in the group receiving aerolized albuterol, while another study of intravenous treatment with salbutamol revealed that use of β_2-agonists could even worsen outcome (Gao Smith *et al.*, 2012, ARDS Network, 2011).

Several groups have reported that animals or isolated lungs pretreated with keratinocyte growth factor (KGF) or KGF-expressing virus particles displayed enhanced Na^+ transport and AFC, and did not develop edema in response to injury (Baba *et al.*, 2007, Morty *et al.*, 2007). It has been demonstrated that transepithelial ion transport is increased in KGF-treated rat AETII cells, which could be attributed to upregulation of *Atp1a1* gene expression and increased Atp1a1 and Atp1b1 protein abundance in these cells (Borok *et al.*, 1998). Similar to KGF, transforming growth factor (TGF)-α also has the capability of improving AFC, albeit through increasing Na^+ uptake as opposed to KGF-induced Na,K-ATPase expression (Folkesson *et al.*, 1996). Additionally, TGF-α-overexpressing mice demonstrate reduced lung edema and decreased mortality in nickel-induced lung injury (Hardie *et al.*, 2002).

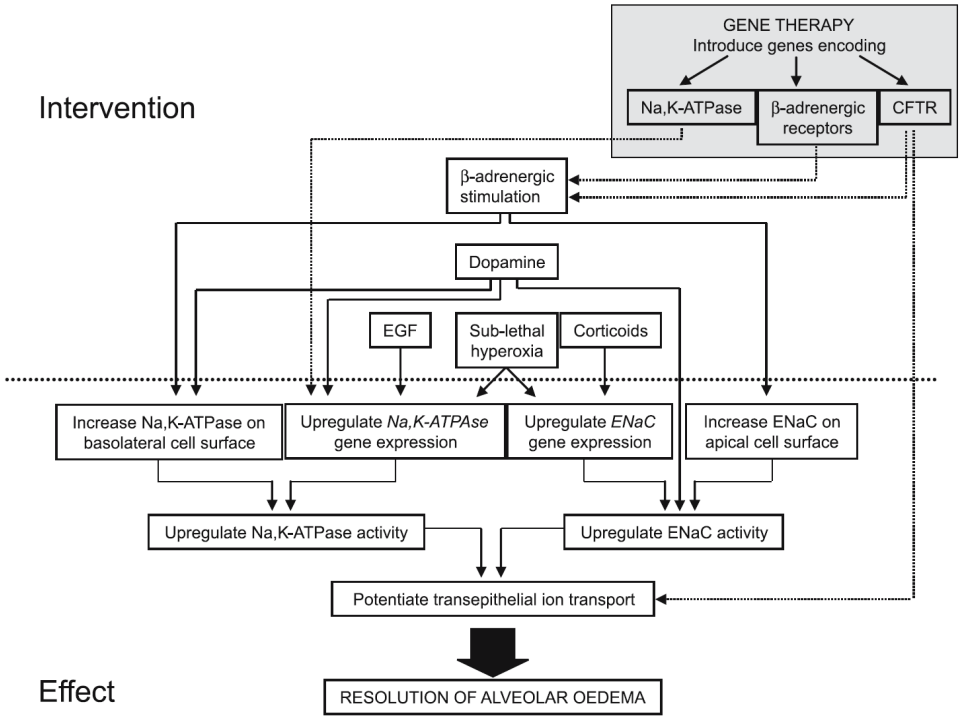

Figure 4. Strategies for improving Na^+ transport and edema resolution in acute respiratory distress syndrome. CFTR, cystic fibrosis transmembrane conductance regulator; EGF, epidermal growth factor (from Morty *et al.*, 2007).

Contrary to routes of indirect stimulation of Na^+ transport, gene therapy by the delivery of Na,K-ATPase subunit-encoding DNA directly augments Na^+ transporting machinery and improves AFC and edema resolution (Adir *et al.*, 2003, Azzam *et al.*, 2002, Stern *et al.*, 2000, Factor *et al.*, 2000, Factor *et al.*, 1998). Interestingly, these experiments proved that increased AFC in ARDS apparently relies on the ATP1B1 subunit (responsible for Na,K-ATPase membrane stability), but not on the ATP1A1 subunit (serving as Na,K-ATPase catalytic centre).

As mentioned above, indirect stimulation of the Na,K-ATPase by TGF-α and KGF, or direct pump augmentation by ATP1B1 subunit overexpression, improved Na^+ transport only in a pretreatment setting, thus limiting the therapeutic potential of these approaches in established ARDS. Moreover, lung protective ventilation with low tidal volumes, the only valid option for ARDS patients, is still not widely employed in intensive care units (Lipes *et al.*, 2012, ARDS Network, 2000). This fact, together with the recently reported ineffectiveness of β_2-agonist therapy, limits possible treatment options for ARDS. The lack of effective treatment options, the overall high mortality and the significant economic burden of ARDS stress the need for the development of new therapeutic strategies. Advances in our understanding of the pathogenesis of this disorder have identified several molecular signaling pathways, including the TGF-β network, which could be potential targets for the future therapy of ARDS.

1.3. Transforming growth factor-β signaling

The members of the TGF-β superfamily of peptide growth factors are evolutionarily conserved amongst vertebrates and regulate embryonic development and organogenesis, wound repair, immune response and hematopoiesis, and control various cell functions (Goumans and Mummery, 2000). The deregulation of TGF-β signaling has been implicated in several lung diseases, including cancer, pulmonary fibrosis, pulmonary arterial hypertension and ARDS (Santibañez *et al.*, 2011, Eickelberg and Morty, 2007, Dhainaut *et al.*, 2003). In alveolar epithelial cells, TGF-β inhibits proliferation, induces apoptosis and epithelial-to-mesenchymal transition (Yamasaki *et al.*, 2008, Willis and Borok, 2007, Zhang *et al.*, 2004,). Secreted in an inactive form and subsequently deposited into extracellular matrix, TGF-β is coupled to latency-associated peptide and latent TGF-β-binding proteins. The availability of TGF-β is tightly controlled and various factors, including proteases (plasmin, matrix

metalloproteinases), reactive oxygen species, integrins and shear forces, have been reported to activate and release the deposited TGF-β (Munger and Sheppard, 2011). The activated TGF-β can be recognized by the cell surface-expressed TGF-β receptor type I (TBRI) and type II (TBRII). The TBRI receptors include activin receptor-like kinase (ALK)1 and ALK5, while TGF-β receptor 2 (TGFBR2) represents the TBRII family. Additionally, auxiliary type III receptors: betaglycan and endoglin, enhance TGF-β signaling by presenting ligand to the TBRI and TBRII complexes (Santibañez *et al.*, 2011). The serine/threonine kinases TBRI/TBRII form the core of the receptor, and upon ligand binding undergo heterodimerization and conformational changes in a series of phosphorylation events (Massagué and Chen, 2000). Initially, recognition of the ligand by TBRII triggers phosphorylation of TBRI followed by reorganization of receptor structure and results in tight association of both molecules. In the subsequent step, TBRI catalyzes the phosphorylation and activation of SMAD proteins (homologs of the *Drosophila* protein mothers against decapentaplegic (MAD) and *Caenorhabditis elegans* protein SMA) which are docked to the receptor complex on cytoplasmatic side (Massagué and Gomis, 2006).

1.3.1. Function of SMAD proteins in the transcriptional regulation of gene expression

In the canonical TGF-β pathway (schematically depicted in Figure 5), activated SMAD2 and SMAD3 proteins form complexes with SMAD4, translocate into the nucleus and act as transcription factors (Massagué and Chen, 2000). Also called receptor SMADs (R-SMADs), SMAD2 and SMAD3 share similar protein structures, with the presence of highly conserved MH1 and MH2 (where MH is Mad homology) domains on the N-terminus and the C-terminus, respectively, separated by linker region. The MH1 domain is responsible for DNA binding while MH2 domain express transcriptional regulation activity and facilitates protein-protein interactions (ten Dijke and Hill, 2004, Ross and Hill, 2008).

Heterodimers consisting R-SMADs and SMAD4 form multiprotein complexes with various transcription factors and transcription co-factors in order to execute the primary function of the TGF-β/SMAD signaling which is gene expression regulation (Massagué and Chen, 2000).

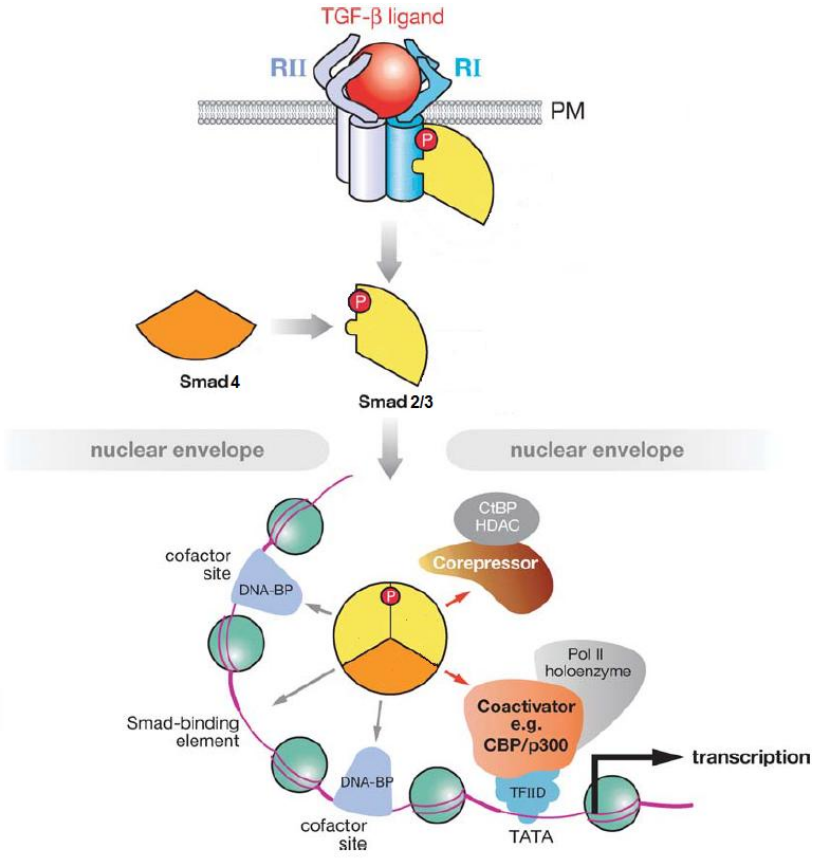

Figure 5. Overview of the TGF-β signaling pathway. CBP, CREB binding protein; CtBP, C-terminal binding protein; DNA-BP, DNA-binding protein; HDAC, histone deacetylase; Pol II, RNA polymerase II; RI, type I receptor; RII, type II receptor; TFIID, transcription factor II D (adapted from Feng and Derynck, 2005).

The intrinsic DNA-binding capability of SMADs is relatively weak and it seems that these proteins do not exhibit strict DNA sequence specificity by binding 5′-AGAC-3′ sequences as well as GC-rich DNA regions, while the most abundant SMAD2 isoform completely lacks DNA-binding activity (Shi *et al.*, 1998, Zawel *et al.*, 1998, Kim *et al.*, 1997). To overcome these drawbacks, SMAD proteins frequently recruit other transcription factors to specifically target and regulate genes downstream of TGF-β signaling. Additionally, as the TGF-β pathway regulates the expression of more than 1300 genes in the human AETII cell-like A549 cell-line alone, these additional transcription factors are necessary to aid the structurally similar SMAD proteins in precise, dynamic and cell-specific gene regulation (Ranganathan *et al.*, 2007, Keating *et al.*, 2006).

1.3.2. SMAD-associated transcription factors and transcription co-factors

A significant number of transcription factors interact and regulate gene expression in concert with SMADs (Feng and Derynck, 2005). The character of the partner transcription factor governs the response to TGF-β and may result in the upregulation or downregulation of target gene expression. The DNA-binding transcription factors known to form transcription-activating complexes with SMADs include forkhead box protein O (FoxO) proteins, specificity protein 1 (Sp1), transcription factor E3 (TFE3) and basic leucine zipper (bZIP) family proteins c-Jun, JunB or activating transcription factor (ATF) 2 and ATF3 (Feng and Derynck, 2005, Seoane *et al.*, 2004, Feng *et al.*, 2000, Hua *et al.*, 1999). Additionally, TGF-β signaling synergizes with NF-kappaB, Notch and p53 pathways (Blokzijl *et al.*, 2003, Cordenonsi *et al.*, 2003, López-Rovira *et al.*, 2000). The primary role of SMADs and partner transcription factors is recognition and binding to specific DNA sequences in the TGF-β target gene promoter. However, the capacity of SMAD proteins to induce transcription is limited, and additional factors, named transcriptional co-activators, are required. The transcriptional co-activators (such as switch/sucrose nonfermentable (SWI/SNF) and ARC105 proteins) lack intrinsic DNA-binding domains but have the ability to modify chromatin structure and stabilize transcriptional machinery, thus significantly amplifying the rate of transcription (Ross *et al.*, 2006, Massagué *et al.*, 2005, Kato *et al.*, 2002).

In contrast to driving gene expression, the mechanisms of TGF-β-dependent gene repression are much less understood, and a number of SMAD-associated transcription factors can play a dual role, acting as a activators as well as repressors, including the already-mentioned p53 (Cordenonsi *et al.*, 2003, Wilkinson *et al.*, 2005). Up to now, several mechanisms of TGF-β/SMAD-regulated gene repression have been described. The gene-activating function of SMADs can be directly suppressed by binding ecotropic virus integration site 1 protein homolog (EVI-1), yin-yang 1 (YY1), Sloan-Kettering institute (SKI) and Ski-related novel protein N (SnoN) transcriptional repressors (Kurisaki *et al.*, 2003, Alliston *et al.*, 2005). Conversely, SMADs may abolish the function of transcriptional activators, as in the case of the interaction between SMAD3 and Runt-related transcription factor 2 (RUNX2) (Alliston *et al.*, 2001). Finally, SMADs may form complexes with specialized transcriptional repressors E2F4

and E2F5 to inhibit gene expression (Chen *et al.*, 2002). Several other transcriptional regulators including transforming growth interacting factor (TGIF), SKI and SNON, can associate with SMADs and may repress the gene expression in a similar fashion (Liberati *et al.*, 2001, Stegmüller *et al.*, 2008, Mizuide *et al.*, 2003, Stroschein *et al.*, 1999, Wotton *et al.*, 1999). Likewise, transcription factor ATF3 associates with SMAD3 in TGF-β-treated epithelial cells and represses the *ID1* gene (Kang *et al.*, 2003). Finally, Vincent and colleagues reported that TGF-β-induces the interaction of SMAD3 and SMAD4 with the transcriptional repressor SNAI1, leading to repression of *CAR*, *OCCLUDIN*, *CLAUDIN-3* and *E-CADHERIN* genes and ultimately epithelial-to-mesenchymal transition (Vincent *et al.*, 2009).

1.3.3. Epigenetic mechanisms in TGF-β-dependent gene regulation

While binding DNA, SMADs and associated transcription factors recruit transcriptional co-activators or co-repressors to finally execute a gene activation or repression program. These two opposite processes may involve epigenetic mechanisms, which modify the accessibility of the eukaryotic transcription machinery by methylating DNA, or by covalently modifying histone proteins. The balance of cytosine methylation in 5′-CG-3′ dinucleotides by DNA methyltransferases and DNA glycosylases is an important mechanism of gene regulation during development. Aberrant DNA methylation patterns have been identified in several diseases including cancer (Wu and Grunstein, 2000). Histone proteins form the core of the nucleosome, the basic structural unit of chromatin, and are responsible for chromatin compacting. Histones are subjected to extensive posttranslational modifications, including lysine acetylation, lysine and arginine methylation, and serine, threonine or tyrosine phosphorylation (Wu and Grunstein, 2000). These covalent modifications alter the histone-DNA interaction and may allow transcription by opening the chromatin structure or facilitate the formation of a closed state of chromatin, which is inaccessible to the transcription machinery. Lysine acetylation plays an important role during the regulation of gene expression, and this modification is characteristic of genes undergoing active transcription. Two types of transcription co-factors control lysine acetylation and, therefore, gene expression:

histone acetyltransferase (HAT) activates while histone deacetylase (HDAC) represses transcription (Wu and Grunstein, 2000).

TGF-β signaling utilizes the function of DNA glycosylases, HAT and HDAC proteins to regulate gene expression. Thillainadesan and colleagues demonstrated that TGF-β induces the interaction between SMAD2-SMAD3 and thymine DNA glycosylase, which conducts active DNA demethylation, activating the $p15^{ink4b}$ gene (Thillainadesan *et al.*, 2012). Several SMAD-interacting proteins exhibit endogenous HAT activity. A study by Kahata and colleagues revealed that a histone H3 acetyltransferase, GCN5, together with SMAD3, localize to the *SERPINE1* gene promoter and activate transcription (Kahata *et al.*, 2004). Moreover, SMAD3, together with SMAD2, forms a complex with another HAT enzyme, p300/CBP-associated factor (PCAF), which amplifies the transcription-inducing properties of SMADs (Kahata *et al.*, 2004, Itoh *et al.*, 2000). Undoubtedly, the nature of the interaction between p300/CBP and SMAD2, SMAD3 and SMAD4 is the most well documented among all SMAD-interacting HATs (Nishihara *et al.*, 1998, Pouponnot *et al.*, 1998). Several TGF-β target genes have been identified to be activated by assembled p300/CBP-SMAD3 or p300/CBP-SMAD4 complexes, including *SERPINE1*, *p15* and the α-2 type I collagen-encoding gene (*COL1A2*) (Ghosh *et al.*, 2000, Shen *et al.*, 1998, Feng *et al.*, 1998).

The HDAC family forms a distinct group of co-repressors operated by TGF-β signaling to downregulate gene expression. Based on homology and cellular localization, this family of zinc-dependent hydrolases is separated into four classes: class I (HDAC1, HDAC2, HDAC3 and HDAC8), class IIa (HDAC4, HDAC5, HDAC7 and HDAC9), class IIb (HDAC6 and HDAC10) and class IV (HDAC11) (Bieliauskas and Pflum, 2008). It has been reported that SMAD3 and SMAD4 directly interact with HDAC1, and protein complexes containing SMADs exhibit histone deacetylation activity (Liberati *et al.*, 2001). The interaction of SMAD3 with HDAC4 and HDAC5 results in repression of the *osteocalcin* gene (Kang *et al.*, 2005). The recruitment of HDAC proteins by SMADs may also be indirect, where other transcription factors serve as adaptors. Evidence provided by Wotton and colleagues demonstrated that TGIF competes with the p300/CBP activator for binding SMAD2, and recruits HDAC1 to the SMAD2-TGIF complex (Wotton *et al.*, 1999). Additionally, SKI and SNON co-repressors seem to recruit HDAC proteins to SMAD-containing complexes. Akiyoshi *et al.* demonstrated that SKI abolishes interaction between SMAD3 and p300 HAT and

recruits HDAC1 to SMAD3 in TGF-β-stimulated cells (Akiyoshi *et al.*, 1999). While SKI-mediated sequestration of HDAC seems to actively antagonize TGF-β/SMAD-mediated induction of at least some genes, SNON maintains the TGF-β target genes in an inactive state under basal conditions. It has been speculated that SNON may recruit HDACs to the SMAD2/SMAD4 complexes *via* the nuclear receptor co-repressor 1 (N-CoR) adaptor protein (Stroschein *et al.*, 1999). The human homolog of *Drosophila* gene *Sna*, SNAI1, represents another transcription factor known to mediate TGF-β signaling, which has also been found to interact with HDACs. Peinado and collaborators described a mechanism where SNAI1, together with HDAC1 and HDAC2, repress *E-Cadherin* gene (Peinado *et al.*, 2004).

1.4. The role of TGF-β signaling in acute respiratory distress syndrome

In the lung, TGF-β is secreted by alveolar macrophages, alveolar epithelial cells and fibroblasts, and is involved in normal lung tissue repair as well as being a critical mediator of pulmonary fibrosis (Khalil *et al.*, 1996, Sime *et al.*, 1997). Additionally, several lines of evidence have implicated TGF-β in processes preceding the development of pulmonary fibrosis. Increased levels of TGF-β have been found in broncho-alveolar lavage (BAL) fluid from ARDS patients and lower levels of TGF-β are related to a lower severity of ARDS (Fahy *et al.*, 2003, Budinger *et al.*, 2005). In ARDS, TGF-β is expressed by fibroblasts, alveolar macrophages and alveolar epithelial cells adjacent to fibrotic foci (Fahy *et al.*, 2003).

The increased levels of TGF-β in BAL fluids from ARDS patients robustly stimulated the activity of the procollagen gene promoter, a fibroproliferative marker and predictor of the severity of ARDS, which could indicate that TGF-β may execute gene regulation programs shortly after the onset of lung injury (Budinger *et al.*, 2005). An analysis of gene expression dynamics in bleomycin- or nickel-induced ARDS models identified a group of TGF-β-target genes involved in the inflammatory response and extracellular matrix deposition to be differentially regulated shortly after the onset of injury. Additionally, the expression of the β-ENaC subunit- and Na,K-ATPase Atp1b1 subunit-encoding genes was decreased, suggesting that disruption of the AFC machinery may occur very early during ARDS progression (Wesselkamper *et al.*, 2005). *In vitro* experiments confirmed that TGF-β boosts vascular endothelial cell permeability, and

decreases transepithelial electrical resistance of primary AETII cells, suggesting a key role for TGF-β signaling in the regulation of ion transport and pulmonary edema formation and persistence in ARDS (Pittet *et al.*, 2001, Hurst *et al.*, 1999). It appears that TGF-β directly targets ENaC channels to perturb ion transport in the lung, as TGF-β treatment decreases α-ENaC subunit-encoding gene expression, and inhibits amiloride-sensitive Na^+ uptake and fluid transport across the alveolar epithelium *in vitro* and *in vivo* (Frank *et al.*, 2003). In contrast, low doses of TGF-β not only preserve α-ENaC subunit encoding gene expression but also increase the abundance of Na,K-ATPase subunits ATP1A1 and ATP1B1, and stimulate active ion transport across AETII cell monolayers (Willis *et al.*, 2003). It is important to note, however, that this effect was accompanied by reduced transepithelial resistance and perturbed formation of tight epithelial monolayers (Willis *et al.*, 2003). Collectively, these observations imply that TGF-β may have a biphasic effect on the epithelial barrier, by stimulating active ion transport at low doses, and disrupting barrier integrity at higher concentrations.

Additional evidence confirming the involvement of TGF-β in ARDS comes from studies where investigators employed tools to block the TGF-β signaling in animal models of ARDS. Pittet and colleagues have suggested a key role of integrin αvβ6 in the local activation of latent TGF-β, since $\alpha v\beta 6^{-/-}$ mice are protected from edema formation, hemorrhage and accumulation of proteinaceous material in the alveoli after bleomycin or endotoxin instillation (Pittet *et al.*, 2001). Additionally, scavenging active TGF-β with a soluble chimeric TGF-β type II receptor decreases protein levels in BAL fluid and epithelial permeability to protein in nickel- and bleomycin-induced lung injury (Pittet *et al.*, 2001, Wesselkamper *et al.*, 2005). However, it is important to note that blocking TGF-β signaling does not affect neutrophil recruitment to the alveoli, suggesting that neutrophil-mediated inflammatory responses are not modulated by TGF-β (Wesselkamper *et al.*, 2005).

Despite the evident involvement of TGF-β in ARDS pathogenesis, functional TGF-β signaling is an important mechanism ensuring organ homeostasis and lung recovery from ARDS. Both inflammation and extracellular matrix modulation are engaged in the tissue repair processes, and are dynamically regulated by TGF-β. In this way, locally deposited TGF-β may be activated by proximal damage and, in response, coordinate securing the perimeter around injured lung tissue and limit the potentially dangerous uncontrolled spread of inflammation (Sheppard, 2006).

2. Hypothesis and aims of the study

The formation and persistence of pulmonary edema is a hallmark of ARDS (Ranieri *et al*., 2012). The resolution of pulmonary edema in ARDS is inhibited by impaired Na^+ transport and insufficient AFC (Sartori and Matthay, 2002). The basolaterally-located Na,K-ATPase establishes an electrochemical gradient across the epithelium which drives osmotic water reabsorption from the alveoli (Matthay *et al.*, 2002). The expression of genes encoding the essential Na,K-ATPase subunit, Atp1b1, has been reported to be reduced in a nickel-induced ARDS model (Wesselkamper *et al*., 2005). Furthermore, TGF-β has been recognized as a key mediator of ARDS pathogenesis, and is known to perturb Na^+ transport and AFC (Wesselkamper *et al.*, 2005, Pittet *et al.*, 2001, Massagué and Chen, 2000). Therefore, it has been hypothesized here that: (i) the expression of Na,K-ATPase encoding genes is deregulated by TGF-β in ARDS patients and in bleomycin model of ARDS in mice; and (ii) restoration of normal expression of genes encoding Na,K-ATPase subunits may improve AFC in the bleomycin model of ARDS.

In detail, the specific aims of this study were:

1. to investigate whether parallel trends in the expression of the Na,K-ATPase subunit-encoding genes exist in the lungs from ARDS patients and in alveolar epithelial cells treated with TGF-β;
2. to elucidate the mechanism of TGF-β-induced regulation of Na,K-ATPase subunit-encoding genes simultaneously regulated in ARDS patients and TGF-β-treated cells;
3. to target and disrupt the gene expression regulatory machinery employed by TGF-β signaling to regulate the Na,K-ATPase subunit-encoding gene expression;
4. to test whether recuperation of the Na,K-ATPase subunit-encoding gene expression may improve alveolar edema status in the bleomycin model of ARDS.

3. Materials and methods

3.1. Materials

3.1.1. Technical equipment

Autoclave; Systec, Germany

Bacteria culture incubator; Heraeus, Germany

Cell culture incubator HERAcell 150i; Thermo Scientific, USA

Cell culture sterile working bench; Thermo Scientific, USA

Cell strainers: 100, 40 μm; BD Falcon™, USA

Centro LB 960 microplate luminometer; Berthold, Germany

Costar® 12 mm Snapwell™ insert; Corning, USA

Countess® cell counter; Invitrogen, UK

Developing machine X Omat 2000; Kodak, USA

Dynal® MX2 sample mixer; Applied Biosystems, USA

Electrophoresis chambers; Bio-Rad, USA

Espresso personal microcentrifuge; VWR, USA

Gel blotting paper; Bioscience, Germany

InoLab® pH meter; WTW, Germany

Isoplate™ B&W 96-well plate; PerkinElmer, USA

Light microscope; Leica, Germany

MicroAmp® 8-tube strip; Applied Biosystems, USA

MicroAmp® FAST 96-well reaction plate; Applied Biosystems, USA

Microcentrifuge tubes: 0.5, 1.5, 2 ml; Eppendorf, Germany

Microsprayer™; Penn-Century Inc, USA

Mini shaker; VWR, USA

Mini Trans-Blot® western blot chambers; Bio-Rad, USA

Mini-Protean® 3 Cell; Bio-Rad, USA

Minispin® centrifuge; Eppendorf, Germany

Multifuge 3 S-R centrifuge; Heraeus, Germany

MS-100 thermo shaker; Universal Labortechnik, Germany

NanoDrop® ND 1000; PeqLab, Germany

Nylon net filters 20 μm; Millipore, USA

peqSTAR 96 universal gradient thermocycler; Peqlab, USA

Petri dishes for bacteria; Greiner Bio-One, Germany

Pipetboy; Eppendorf, Germany

Pipetmans: P10, P20, P100, P200, P1000; Gilson, France

Pipetman filter tips: 10, 20, 100, 200 and 1000 µl; Greiner Bio-One, Germany

Precellys® 24 homogenizer; Bertin Technologies, France

Refrigerated microcentrifuge CT15RE; VWR, USA

Serological pipettes: 2, 5, 10, 25, 50 ml; Falcon, USA

Sonopuls HD 2070 ultrasonic homogenizer; Bandelin, Germany

StepOnePlus™ Real-Time PCR system; Applied Biosystems, USA

Test tubes: 15, 50 ml; Greiner Bio-One, Germany

Tissue culture dish 100 mm; Greiner Bio-One, Germany

Tissue culture flask 250 ml; Greiner Bio-One, Germany

Tissue culture plates: 6-, 12-, 48- and 96-well; Greiner Bio-One, Germany

Tissue culture plates: 12-well; Greiner Bio-One, Germany

Tissue culture plates: 48-well; Greiner Bio-One, Germany

Tissue culture plates: 96-well; Greiner Bio-One, Germany

Transfer membrane nitrocellulose; Bio-Rad, USA

Vasofix® Safety intravenous catheter; B. Braun, Germany

VersaMax micro-plate reader; Molecular Devices, USA

Vortex mixer; VWR, USA

3.1.2. Chemicals and reagents

2-Propanol; Merck, Germany

5-Aza-2′deoxycytidine; Sigma-Aldrich, Germany

Agarose; Promega, Germany

Agarose, low melting point; Sigma-Aldrich, Germany

Anti-CD16/32 antibody; BD Biosciences, USA

Anti-CD31 antibody; BD Biosciences, USA

Anti-CD45 antibody; BD Biosciences, USA

Anti-HDAC2 antibody (chromatin immunoprecipitation); Pierce Biotechnology, USA

Ammonium chloride; Sigma-Aldrich, Germany

Ammonium persulfate; Promega, Germany

Ampicillin sodium salt; Sigma-Aldrich, Germany

Bovine serum albumin; Sigma-Aldrich, Germany

Bromophenol blue; Sigma-Aldrich, Germany

Calcium chloride; Sigma-Aldrich, Germany

Complete™ protease inhibitor; Roche, Germany

Deoxycholate; Sigma-Aldrich, Germany

Dispase; BD Biosciences, USA

3,3′-Dithiodipropionic acid di(N-hydroxysuccinimide ester); Sigma-Aldrich, Germany

DMSO; Sigma-Aldrich, Germany

DNase I; Serva, Germany

dNTP mix; Promega, USA

DTT; Promega, USA

Dual-Luciferase® reporter assay system; Promega, USA

Dulbecco's modified Eagle's medium; Gibco BRL, Germany

Dulbecco's modified Eagle's medium, high glucose; Gibco BRL, Germany

Dulbecco's phosphate buffered saline, 10×; PAA Laboratories, Austria

Dulbecco's phosphate buffered saline, 1×; PAA Laboratories, Austria

Dynabeads®, streptavidin-coupled; Invitrogen, UK

EDTA; Sigma-Aldrich, Germany

EGTA; Sigma-Aldrich, Germany

Ethanol 70%; SAV-LP, Germany

Ethanol 99%; J.T. Baker Mallinckrodt Baker B.V., Netherlands

Ethanol absolute; Riedel-de Haën, Germany

Ethidium bromide; Promega, USA

Evans blue; Sigma-Aldrich, Germany

Fetal calf serum; PAA Laboratories, Austria

Formaldehyde, 37%; Sigma-Aldrich, Germany

Formamide; Fluka, Germany

Giemsa's azur eosin methylene blue solution; Merck, Germany

Glycerol; Carl Roth, Germany

Glycine; Carl Roth, Germany

Hank's balanced salt solution; PAA Laboratories, Austria

HEPES; PAA Laboratories, Austria

*Hin*dIII restriction enzyme; Promega, USA

Hydrochloric acid; Sigma-Aldrich, Germany

Igepal® CA-630; Sigma-Aldrich, Germany

Isoflurane; CP-Pharma, Germany

Ketamine; Pharmacia & Upjohn, Sweden

Lipofectamine™ 2000; Invitrogen, UK

Lithium chloride; Sigma-Aldrich, Germany

Luria-Bertani medium; Invitrogen, UK

Magnesium chloride; Sigma-Aldrich, Germany

Magnesium chloride, 25 mM; Applied Biosystems, USA

May-Grünwald's eosin-methylene blue solution; Merck, Germany

MC1568; Sigma-Aldrich, Germany

β-Mercaptoethanol; Sigma-Aldrich, Germany

Methanol; Fluka, Germany

MGCD0103; Selleck Chemicals, USA

MuLV reverse transcriptase; Applied Biosystems, USA

Non-fat dry milk; Carl Roth, Germany

Normal rabbit IgG; Santa Cruz Biotechnology, USA

NucleoBond® Xtra midi plasmid midiprep kit; Macherery-Nagel, Germany

NucleoSpin® RNA II kit; Macherery-Nagel, Germany

Nuclease-free water; Ambion, USA

Opti-MEM® medium; Gibco BRL, Germany

Passive lysis buffer; Promega, USA

PCR buffer II, 10×; Applied Biosystems, USA

Penicillin/streptomycin solution; PAA Laboratories, Austria

pGL3-Basic; Promega, USA

Platinum® SYBR® Green qPCR SuperMix UDG kit; Invitrogen, USA

Pierce® BCA protein assay kit; Thermo Scientific, USA

Potassium bicarbonate; Sigma-Aldrich, Germany

Precision Plus Protein™ standards; Bio-Rad, USA

pRL-SV40; Promega, USA

Protein A/G PLUS-agarose; Santa Cruz Biotechnology, USA

Proteinase K; Promega, USA

QIAquick gel extraction kit; Qiagen, Netherlands

QIAquick PCR purification kit; Qiagen, Netherlands

Quick Start™ Bradford dye reagent; Bio-Rad, USA

Random hexamers; Applied Biosystems, USA

RIPA buffer; Thermo Scientific, USA

RNase inhibitor; Applied Biosystems, USA

Rompun®; Bayer, Germany

Rotiphorese Gel 30 acrylamide/bisacrylamide mixture; Carl Roth, Germany

*Sac*I restriction enzyme; Promega, USA

SB431542; Calbiochem, USA

SDS, 10% solution; Promega, USA

SDS, powder; Carl Roth, Germany

Select agar; Sigma-Aldrich, Germany

Sonicated salmon sperm DNA; Agilent, USA

Sodium acetate; Sigma-Aldrich, Germany

Sodium bicarbonate; Sigma-Aldrich, Germany

Sodium chloride; Merck, Germany

Sodium orthovanadate; Sigma-Aldrich, Germany

Sodium phosphate; Sigma-Aldrich, Germany

Sodium sulfate; Merck, Germany

SuperSignal® West Femto chemiluminescent substrate; Thermo Scientific, USA

TEMED; Bio-Rad, USA

TGF-β1; R&D Systems, USA

Trichostatin A; Sigma-Aldrich, Germany

Tris; Carl Roth, Germany

Triton X-100; Promega, USA

TRIzol® reagent; Ambion, USA

Trypan blue; Fluka, Germany

Trypsin/EDTA; Gibco BRL, Germany

Tween® 20; Sigma-Aldrich, Germany

3.1.3. Cell lines

A549 epithelial cell line, human lung adenocarcinoma; ATCC-LGC, Germany

3.2. Methods

3.2.1. Human lung material

All investigations involving human material were approved by the University of Giessen Ethics Committee (approval number 29/01). Lung tissue was collected at autopsy from five ARDS patients, and from four patients who died of myocardial infarction, with no signs of pulmonary disease. Patients with ARDS met all American-European consensus conference on ARDS clinical criteria and required mechanical ventilation for a mean duration of 92 h. The clinical characteristics of these patients are presented in Table 1.

Table 1. The clinical characteristics of acute respiratory distress syndrome patients.

Patient	Age	Sex	Background	Modified APACHE II	PaO_2/FiO_2 (mmHg)
1	40	female	Pneumonia	11	83.0
2	51	female	Trauma	6	181.5
3	48	female	Pancreatitis	20	127.2
4	59	female	Trauma	16	137.1
5	67	male	Sepsis	20	109.0

Abbreviations: APACHE, acute physiology and chronic health evaluation; FiO_2, fraction of inspired oxygen; PaO_2, partial pressure of oxygen in arterial blood.

3.2.2. *ATP1B1* promoter cloning

3.2.2.1. Sub-cloning of the *ATP1B1* promoter from the pGEM-T Easy vector into the pGL3-Basic vector

The pGEM-T Easy-*ATP1B1*-promoter plasmid containing a 1837-base-pair (bp) fragment of the *ATP1B1* gene promoter (-3075 to -1238 bp upstream from transcription start site) was created by Verena Arnoldt. In order to clone the *ATP1B1* promoter into the firefly luciferase reporter vector pGL3-Basic, 0.2 µg of the pGEM-T Easy-*ATP1B1*-promoter plasmid was digested with *Hin*dIII and *Sac*I restriction enzymes (6 units of each enzyme was used per reaction) for 1 h at 37 °C.

Products of restriction were then analyzed on a 1.5% agarose gel containing 0.5 µg ethidium bromide. A single band migrating at approximately 1800 bp corresponding to the *ATP1B1* promoter was then excised with a clean scalpel and purified using a QIAquick gel extraction kit according to the manufacturer instructions. Next, 100 ng of the *ATP1B1* promoter DNA was mixed with 50 ng pGL3-Basic vector (previously digested with *Hin*dIII and *Sac*I restriction enzymes) and ligated using T4 DNA Ligase at 4 °C overnight, thereby creating the pGL3-Basic-*ATP1B1*-promoter construct.

3.2.2.2. Plasmid transformation of competent cells

The XL1-Blue competent bacteria cells were transformed using a heat shock transformation protocol. Bacterial suspension (50 µl) was transferred into a 1.5 ml tube containing 2 µl of the ligation mixture (30 ng of DNA) and incubated for 20 min on ice. Next, bacteria were subjected to heat shock at 42 °C for 45 s and the tube was immediately transferred back to ice for 2 min. Then, 950 µl of Luria-Bertani medium (LB-medium) was added, and the tube was incubated at 37 °C for 1.5 h with shaking at 150 revolutions per minute (rpm). Thereafter, tubes were centrifuged at 3000 rpm for 5 min at room temperature (RT), after which, the supernatant was discarded and the bacterial pellet was resuspended in 100 µl of LB-medium. The bacterial suspension was then plated on LB-agar supplemented with 50 µg/ml ampicillin and incubated at 37 °C overnight.

3.2.2.3. Plasmid midi-preparation

A single bacteria colony was inoculated into 5 ml of LB-medium supplemented with 50 µg/ml ampicillin, and incubated for 8 h at 37 °C with shaking at 180 rpm. Thereafter, 2 ml of the bacterial pre-culture was transferred into an Ehrlenmeyer flask containing 200 ml of LB-medium supplemented with 50 µg/ml ampicillin and incubated overnight at 37 °C with shaking at 180 rpm. The pGL3-Basic-*ATP1B1*-promoter plasmid was then extracted from the bacteria culture using a NucleoBond® Xtra Midi kit according to the manufacturer's instructions.

3.2.3. A549 cell culture

The human lung adenocarcinoma epithelial cell line A549 was cultured in tissue culture flasks in Dulbecco's modified Eagle's medium (DMEM) supplemented with 10% fetal calf serum (FCS) at 37 °C, 5% CO_2 and 95-100% humidity. After 80-90% confluence was reached, cells were subcultured using a single wash with phosphate buffered saline (PBS) followed by incubation with 3 ml Trypsin-EDTA solution for 3 min at 37 °C. The trypsin activity was inhibited with 7 ml of DMEM containing 10% FCS. Next, the cell suspension was diluted 1:5 with DMEM medium supplemented with 10% FCS and transferred into the fresh tissue culture flask.

3.2.3.1. Treatment of A549 cells

The A549 cells were treated with 0, 2, 6 or 10 ng/ml TGF-β1 for 1, 2, 3, 24 or 48 h. Inhibition of TGF-β signaling pathway was achieved by use of SB431542 (20 μM) added to the media 1 h before TGF-β1 treatment. Inhibition of DNA methylation was achieved by use of 0.1 μM or 10 μM 5-Aza-2′deoxycytidine (5-Aza-2′-dC) added to the media 24 h before beginning of TGF-β1 stimulation, and replenished every 24 h over the duration of the experiment. Trichostatin A (TSA, 64 nM), MGCD0103 (10 μM) and MC1568 (10 or 20 μM) histone deacetylase inhibitors were added 24 h after TGF-β1 was introduced and were left for another 24 h.

3.2.3.2. Transient transfection of short interfering RNA

The Lipofectamine™ 2000 transfection reagent was used to transiently transfect A549 cells with siRNA. Cells were seeded one day prior transfection into a 12-well plate, and were 40-50% confluent at the time of transfection. In order to transfect the cells with 100 nM siRNA, 2 μl of Lipofectamine™ 2000 regent was added to 50 μl of Opti-MEM® serum-free medium and left for 5 h at RT. Next, siRNA oligonucleotides (listed in Table 2) dissolved in Opti-MEM® medium were added, and incubated for 20 min at RT. For transfection of cells with 200 nM siRNA, 4 μl of Lipofectamine™ 2000 regent was used. The transfection mixture was then added to the cells cultured in the DMEM medium supplemented with 10% FCS. Cells were cultured for 24, 48, 72 or 96 h under normal cell culture conditions or exposed to 10 ng/ml TGF-β1 after 24 or 48 h for additional 48 h.

Table 2. List of siRNA oligonucleotides used in knock-down experiments.

Target gene	Company	Catalog number
E2F4	Santa Cruz Biotechnology, USA	sc-29300
E2F5	Santa Cruz Biotechnology, USA	sc-35250
HDAC1	Invitrogen, USA	1299001/HSS104725
HDAC2	Invitrogen, USA	1299001/HSS104728
HDAC3	Santa Cruz Biotechnology, USA	sc-35538
RUNX2	Qiagen, Netherlands	SI00063000
scrambled siRNA	Ambion, USA	AM4611
SMAD2	Santa Cruz Biotechnology, USA	sc-44338
SMAD3	Santa Cruz Biotechnology, USA	sc-38376
SMAD4	Santa Cruz Biotechnology, USA	sc-29484
SNAI1	Santa Cruz Biotechnology, USA	sc-38398
SNON	Santa Cruz Biotechnology, USA	sc-36518
YY1	Santa Cruz Biotechnology, USA	sc-36863

3.2.3.3. Transient transfection of DNA

The A549 cells were transiently transfected with DNA using Lipofectamine™ 2000 transfection reagent. Cells were seeded into a 48-well plate and incubated until a confluence of 50% was achieved. To transfect the cells, 0.75 μl of Lipofectamine™ 2000 regent was mixed with 49.25 μl of Opti-MEM® serum-free medium and left for 5 min at RT. This mixture was then combined with solution containing 300 ng of pGL3-Basic-*ATP1B1*-promoter firefly luciferase reporter combined with 7 ng of pRL-SV40 *Renilla* luciferase co-reporter plasmid in 48.2 μl of Opti-MEM® medium and incubated for 20 min. Thereafter, culture medium was exchanged with transfection mixture and cells were left for 5 h. Next, transfection medium was aspirated, fresh DMEM medium supplemented with 10% FCS was added, and cells were left for 48 h under normal cell culture conditions, or treated with 0, 2, 6 or 10 ng/ml TGF-β1. When histone deacetylation was studied, 64 nM TSA, 10 μM MGCD0103 or 10 μM MC1568 inhibitors were added 24 h after TGF-β1 was introduced. In the case of DNA methylation inhibition, 0.1 or 10 μM 5-Aza-2′-dC was added 24 h before transfection, and was reintroduced every 24 h.

3.2.4. Culture of primary mouse alveolar epithelial type II cells

3.2.4.1. Isolation of primary mouse alveolar epithelial type II cells

Primary AETII cells were isolated using the modified protocol published by Corti and collaborators (Corti *et al.*, 1996). Adult male C57BL/6J mice were anesthetized with isoflurane. The abdomen was opened by midline incision and mice were exsanguinated by transection of the *Arteria renalis*. The diaphragm was then punctured, and after the lung was retracted, the chest was opened and the ribs were fixed laterally. The left atrium was then punctured and the lungs were perfused with Hank's balanced salt solution *via* the right ventricle. The trachea was cannulated with a Vasofix® Safety intravenous catheter and 2 ml of dispase followed by 0.5 ml of 1% low-melting point agarose was injected to the lungs. After 5 min, the lungs were removed, transferred into 2 ml of dispase and incubated for 45 min at RT. The lungs were dissected in 7 ml of DMEM medium without FCS (supplemented with 0.01% DNase I) and incubated for 10 min at RT. The resulting crude cell suspension was sequentially filtered through 100-µm and 40-µm cell strainers followed by final filtration through 20-µm nylon mesh. The filtrate was then centrifuged at 130 g for 8 min at 4 °C and resuspended in 7 ml of erythrocyte lysis buffer and incubated for 5 min at RT. Erythrocyte lysis was stopped with 7 ml of PBS, cells were centrifuged at 130 g for 8 min at 4 °C and resuspended in 5 ml DMEM medium containing 10% FCS. The cells were then stained with trypan blue, counted using a Countess® Cell Counter and incubated with 0.75 µl biotinylated anti-CD16/32, 0.9 µl biotinylated anti-CD45 and 0.4 µl biotinylated anti-CD31 antibodies per 1 million cells, for 30 min at 37 °C. The cells were then washed with 5 ml of DMEM medium without FCS, and AETII cells were negatively selected using streptavidin-coupled Dynabeads® for 30 min at RT with gentle mixing followed by final centrifugation at 130 g for 8 min at 4 °C and resuspension in DMEM medium with 10% FCS.

DMEM medium without FCS	**Erythrocyte lysis buffer**
DMEM high glucose medium	0.1 mM Na_2EDTA, pH 7.4
10 mM HEPES, pH 7.2	0.154 M NH_4Cl
1% penicillin/streptomycin solution	10 mM $KHCO_3$

DMEM medium with 10% FCS

DMEM high glucose medium

10 mM HEPES, pH 7.2

1% penicillin/streptomycin solution

10% FCS

3.2.4.2. Treatment of primary mouse alveolar epithelial type II cells

The AETII cells were seeded on 12 mm diameter Snapwell™ inserts at a density of 5×10^5 cells/well. After 24 h, the culture medium was removed from the apical compartment and the cells were grown under the air-liquid conditions. The cells were then treated with 10 ng/ml TGF-β1 for 48 h. For HDAC inhibition, 64 nM TSA, 10 μM MGCD0103 or 10 μM MC1568 was added 24 h after TGF-β1 was introduced and incubated for another 24 h.

3.2.5. Dual-luciferase reporter assay

Firefly and *Renilla* luciferase activity in A549 cells transiently co-transfected with pGL3-Basic-*ATP1B1*-promoter firefly reporter and pRL-SV40 *Renilla* firefly co-reporter vectors was measured using the Dual-Luciferase® reporter assay system. The co-transfected cells were lysed in 100 μl passive lysis buffer for 10 min in RT, with shaking at 100 rpm. Next, 5 μl of the cell lysate was transferred into 96-well plate, loaded into a Centro LB 960 microplate luminometer, and the activities of firefly and *Renilla* luciferases were measured sequentially in each well. The luminescence measurement protocol was as follows: dispersion of 50 μl of LAR II reagent (firefly luciferase substrate), quantification of luminescence for 7 s, dispersion of 50 μl Stop & Glo® regent (containing inhibitor of firefly luciferase and substrate for *Renilla* luciferase) and quantification of luminescence for 7 s. The *ATP1B1* promoter activity was expressed as ratio of firefly-to-*Renilla* luciferase luminescence signals.

3.2.6. Gene expression analysis

3.2.6.1. RNA isolation from lung tissue and from cell culture

Total lung RNA was isolated from 70-90 mg of tissue using 1 ml of TRIzol® reagent per 100 mg tissue. Lung tissue was homogenized in a Precellys®

24 homogenizer. Subsequently, 0.2 ml chloroform per 1 ml TRIzol® reagent used for homogenization was added and samples were centrifuged at 12000 g for 15 min at 4 °C. After phase separation, the aqueous phase was transferred into a fresh 1.5 ml tube, and samples were combined with 0.5 ml 2-Propanol per 1 ml TRIzol® reagent used for homogenization, and left for 10 min at RT. Next, samples were centrifuged at 12000 g for 10 min at 4 °C, the supernatant was removed and the RNA pellet was washed once with 1 ml of 75% ethanol. Quantification and purity of the isolated RNA was determined with a NanoDrop® ND 1000. The cDNA was synthesized from RNA preparations with $A_{260/280}$ absorbance ratio above 1.90.

The total RNA from cells in culture was isolated using a NucleoSpin® RNA II kit according to the manufacturer's instructions. The quantification and purity of isolated RNA was determined with a NanoDrop® ND 1000. The cDNA was synthesized from RNA preparations with $A_{260/280}$ absorbance ratio above 1.90.

3.2.6.2. cDNA synthesis

Reverse transcription was performed on 500 ng of total RNA using MuLV reverse transcriptase and random hexamer oligodeoxyribonucleotides. To perform cDNA synthesis, 20 µl of RNA was denatured at 70 °C for 10 min, transferred onto ice, and supplemented with 20 µl of reverse transcription mixture. Afterwards, the mixture was incubated at 21 °C for 10 min, followed by an RNA synthesis step at 43 °C for 1 h 15 min. The final incubation at 99 °C for 5 min was performed to inactivate MuLV reverse transcriptase.

Reverse transcription mixture	
10× PCR buffer II	4 µl
25 mM $MgCl_2$	8 µl
H_2O	1 µl
Random hexamers	2 µl
RNase inhibitor	1 µl
10 nM dNTP mix	2 µl
MuLV reverse transcriptase	2 µl
Total volume	20 µl

3.2.6.3. Real-time quantitative PCR

Analysis of the gene expression at the mRNA level was performed by real-time quantitative polymerase chain reaction (qPCR) using a Platinum® SYBR® Green qPCR SuperMix UDG kit and a StepOnePlus™ Real-Time PCR System. Intron-spanning primer pairs specific to the target mRNA were designed using Primer-BLAST software (http://www.ncbi.nlm.nih.gov/tools/primer-blast/). Primers used in the gene expression analyses are listed in Table 3.

Table 3. Primers used for gene expression analysis.

Gene	Species	Forward and reverse primers sequences
ATP1A1	human	5′-AGCTACCTGGCTTGCTCTGTCC-3′ 5′-GCTGACTCAGAGGCATCTCCTGC-3′
ATP1B1	human	5′-AAAAGTACAAAGATTCAGCCCAGAGGG-3′ 5′-AGCTTGAATCTGCAGACCTTTCGC-3′
Atp1b1	mouse	5′-CCCAAGAGCTACGAGGCCTACG-3′ 5′-GTCGCCCCGTTCCTTGGGTTC-3′
FXYD1	human	5′-TCGCCGGGATCCTCTTCATCC-3′ 5′-CCCTCCTCTTCATCGGGTTCCCC-3′
FXYD2	human	5′-AATGGGGGCCTGATCTTC-3′ 5′-CTTCTTATTGCCCCCACAGC-3′
FXYD3	human	5′-AGCGCTCTGACATGCAGAAGGTG-3′ 5′-TCTTCTAGGTCATTGGCGTCCAGG-3′
FXYD4	human	5′-GCGGACTGATCTGCGGAGGG-3′ 5′-GCTGCTTCTGGCTGCTCTTGC-3′
FXYD5	human	5′-AGCAACTGGAAGGAACGGAT-3′ 5′-GGGTCTGTCTGGACGTCTGT-3′
FXYD6	human	5′-CCCCAGAAAGCAGAGAACTG-3′ 5′-GGCCGGTTTTCTTAAGCATC-3′
FXYD7	human	5′-TGTGGGCATGACTCTGGCAACC-3′ 5′-TGGAGTCCGCCTTCCTGCAC-3′
HPRT1	human	5′-AAGGACCCCACGAAGTGTTG-3′ 5′-GGCTTTGTATTTTGCTTTTCCA-3′
Hprt1	mouse	5′-GCTGACCTGCTGGATTAC-3′ 5′-TTGGGGCTGTACTGCTTA-3′

The thermal cycling conditions were as follows: 50 °C for 2 min, 95 °C for 5 min, 40 cycles of 95 °C for 5 s, 59 °C for 5 s, 72 °C for 30 s. The samples were then subjected to melting curve analysis to ensure amplification of a single, specific product and to exclude the possibility of primer-dimer formation. A constitutively expressed human *HPRT1* or mouse *Hprt1* reference gene was used as a reference gene for qPCR reactions. Target gene expression was assessed with the comparative Ct method (ΔCt method) and calculated with the equation: $\Delta Ct = Ct_{HPRT1} - Ct_{target}$.

3.2.7. Protein expression analysis

3.2.7.1. Protein isolation

The entire protein isolation procedure was carried out on ice to prevent protein degradation. Protein lysis buffer was supplemented with 1 mM sodium orthovanadate and Complete™ protease inhibitor cocktail (1 tablet per 25 ml of protein lysis buffer) immediately before use. Next, 100 µl or 200 µl of protein lysis buffer was added to the A549 cells seeded on 6-well or 12-well plates, respectively, and cells were collected with a cell scraper into a 1.5 ml tube and incubated for 30 min with occasional vortexing. Tubes were then centrifuged at 13000 rpm for 15 min at 4 °C and the supernatant was then transferred into fresh 0.5 ml tubes. To measure protein concentration, samples as well as protein lysis buffer were diluted 1:10 with water and 10 µl was transferred into a 96-well plate. In parallel, a series of 10 µl of bovine serum albumin protein standards were included on the same plate. Subsequently, 100 µl of Quick Start™ Bradford dye regent was added to each well, plate was left for 5 min and the absorbance was measured at a 570 nm wavelength using a VersaMax micro-plate reader. Protein concentrations were calculated for each sample using a standard curve.

Protein lysis buffer

150 mM NaCl

1 mM EDTA

1 mM EGTA

0.5% Igepal® CA-630

20 mM Tris-Cl, pH 7.5

3.2.7.2. Protein electrophoresis and western blot

Protein samples were mixed with 10× sample buffer and resolved by sodium dodecyl sulfate polyacrylamide gel electrophoresis at 110 mV in running buffer. After the bromophenol blue tracking dye had left the resolving gel, proteins were blotted onto a nitrocellulose membrane at 110 mV for 1 h in blotting buffer. Next, the membrane was washed once with washing buffer and incubated for 1 h in blocking buffer at RT. Membranes were then incubated with primary antibody diluted in blocking buffer at 4 °C overnight. Primary antibodies used in the western blot analysis are listed in Table 4. After the membrane was rinsed in washing buffer four times for 3 min each, the

horseradish peroxidase-conjugated secondary antibody diluted in blocking buffer was then added, and the membrane was incubated for 1 h at RT. Thereafter, the membrane was rinsed four times for 3 min each in washing buffer, and was incubated in SuperSignal® West Femto chemiluminescent substrate for 3 min at RT. The protein bands were visualized and archived with a LAS-4000 luminescent image analyzer.

Table 4. Primary antibodies used in western blot analysis.

Antibody	Dilution	Company	Catalog number
Anti-β-ACTIN	1:1000	Cell Signaling Technology, USA	4967L
Anti-E2F4	1:100	Santa Cruz Biotechnology, USA	sc-1082
Anti-E2F5	1:100	Santa Cruz Biotechnology, USA	sc-999
Anti-HDAC1	1:500	Cell Signaling Technology, USA	2062
Anti-HDAC2	1:500	Santa Cruz Biotechnology, USA	sc-6296
Anti-HDAC2 (phospho S394)	1:500	Abcam, UK	ab75602
Anti-HDAC3	1:500	Santa Cruz Biotechnology, USA	sc-8138
Anti-LAMIN A/C	1:5000	Santa Cruz Biotechnology, USA	sc-20681
Anti-RUNX2	1:500	Invitrogen, USA	41-1400
Anti-SMAD2	1:1000	Cell Signaling Technology, USA	3103
Anti-SMAD2 (phospho S465/467)	1:1000	Cell Signaling Technology, USA	3101S
Anti-SMAD3	1:1000	Cell Signaling Technology, USA	3102
Anti-SMAD3 (phospho S423/425)	1:1000	Cell Signaling Technology, USA	9520S
Anti-SMAD4	1:500	Cell Signaling Technology, USA	9515
Anti-SNAI1	1:500	R&D Systems, USA	AF3639
Anti-SNON	1:500	Cell Signaling Technology, USA	4973
Anti-YY1	1:500	Santa Cruz Biotechnology, USA	sc-7341

10× Sample buffer

650 mM Tris-Cl, pH 6.8
1 mM EDTA
50% glycerol
0.3% bromophenol blue
9% β-mercaptoethanol

10% Resolving gel

10% acrylamide/bisacrylamide mixture
375 mM Tris-Cl, pH 8.8
0.05% SDS
0.05% APS
0.065% TEMED

Stacking gel
5% acrylamide/bisacrylamide mixture
125 mM Tris-Cl, pH 6.8
0.05% SDS
0.05% APS
0.065% TEMED

Blotting buffer
25 mM Tris-Cl, pH 8.3
192 mM glycine
20% methanol

Running buffer
250 mM Tris-Cl, pH 8.3
2.5 M glycine
1% SDS

Washing buffer
1× PBS, pH 7.2
0.1% Tween® 20

Blocking buffer
1× PBS, pH 7.2
0.1% Tween® 20
5% non-fat dry milk

3.2.8. Chromatin immunoprecipitation

Chromatin immunoprecipitation (ChIP) assay was performed on A549 cells plated on 60 mm dishes. Cells were cultured until 90% confluence was reached and stimulated with 10 ng/ml TGF-β1 for 3 h. Cells were then washed with PBS twice, and subjected to dual cross-linking with 1 mM 3,3′-Dithiodipropionic acid di(N-hydroxysuccinimide ester) (DSP) in PBS for 30 min followed by incubation with 1% formaldehyde for 10 min at RT, with shaking at 100 rpm. Cross-linking was quenched with 125 mM glycine for 5 min at RT. After a single washing step with PBS, the procedure was carried out on ice to prevent the degradation of protein and DNA. Cells were lysed for 10 min in 1 ml of RIPA buffer supplemented with 1 mM sodium orthovanadate and Complete™ protease inhibitor cocktail (1 tablet per 25 ml of RIPA buffer). The lysate was collected with a cell scraper into a 1.5 ml tube and chromatin was sheared into 200-300 bp-long fragments using a Sonopuls HD 2070 ultrasonic homogenizer using the following settings: 7 rounds of 10 pulses with 40% duty cycle and 40% power output settings. The lysate was then centrifuged at 14000 rpm for 15 min, and the supernatant was collected. The 163 µl of supernatant was diluted 1:6 in RIPA buffer and pre-cleared with 50 µl protein A/G agarose beads saturated with 10 µg of sonicated salmon sperm DNA for 1 h with gentle orbital rotation. After the centrifugation at 3000 rpm for 4 min, protein A/G agarose beads were discarded, and the immunoprecipitation was carried out with 20 µg of anti-HDAC2 or normal rabbit IgG

antibodies added to the pre-cleared chromatin lysate. Two hours later, 50 µl protein A/G agarose beads saturated with 10 µg of sonicated salmon sperm DNA was added and left overnight with gentle orbital rotation. Antibody-chromatin complexes conjugated to protein A/G agarose beads were then sequentially washed with 1 ml of low salt buffer, 1 ml high salt buffer, 1 ml LiCl buffer and twice with 1 ml TE buffer. Each washing step was conducted for 5 min followed by centrifugation at 3000 rpm for 3 min at RT and removal of the supernatant. To elute antibody-chromatin complexes, 150 µl elution buffer was added and samples were incubated for 30 min at 65 °C with shaking at 500 rpm. Samples were centrifuged at 3000 rpm for 3 min at RT and the supernatant was saved in a fresh 1.5 ml tube. To test the efficiency of the antibody to immunoprecipitate HDAC2, 36 µl of eluate or input samples was subjected to protein electrophoresis and western blot as described above. To purify DNA from protein, immunoprecipitated chromatin was reverse cross-linked at 65 °C followed by addition of 50 mM DTT and incubation for 30 min at 37 °C and 0.5 µg/ml proteinase K treatment for 30 min at 55 °C. The DNA was further purified using QIAquick PCR purification kit according to the manufacturer instructions. Semi-quantitative PCR and qPCR were then performed using Platinum® SYBR® Green qPCR SuperMix UDG kit on 4 ng of DNA. Primers used in the ChIP experiments are listed in Table 5. The product of the semi-quantitative PCR were resolved on 3% agarose gel containing 0.5 µg ethidium bromide and archived using X Omat 2000 developer.

Low salt buffer
0.1% SDS
1% Triton X-100
2 mM EDTA
20 mM Tris-Cl, pH 8.0
150 mM NaCl

High salt buffer
0.1% SDS
1% Triton X-100
2 mM EDTA
20 mM Tris-Cl, pH 8.0
500 mM NaCl

LiCl buffer
0.25 M LiCl
1% Igepal® CA-630
1% deoxycholate
1 mM EDTA
10 mM Tris-Cl, pH 8.0

TE buffer
1 mM EDTA
10 mM Tris-Cl, pH 8.0

Elution buffer
1% SDS, pH 8.0
0.1 M $NaHCO_3$, pH 8.0

Table 5. Primers used in chromatin immunoprecipitation experiments.

Locus	Forward and reverse primers sequences
ATP1B1 promoter	5′-CCCCCAAGGGGGCATAAAAGCA-3′ 5′-AGGCACAATATCTGCACGTGACC-3′
HPRT1 exon three	5′-ACGTCTTGCTCGAGATGTGAT-3′ 5′-GATGTAATCCAGCAGGTCAGC-3′

3.2.9. Animal experiments

3.2.9.1. The bleomycin model of acute respiratory distress syndrome and trichostatin A treatment

Animal experiments were approved by local authorities (Regierungspräsidium Darmstadt, approval number B 2/281). Male mice (C57BL/6J) were obtained from Charles River Laboratories, Sulzfeld, Germany. Only animals weighing 20-25 g were used in the study. Mice were anesthetized with mixture of 100 mg ketamine per kg body weight and 8 mg xylazine per kg body weight. Thereafter, mice were orotracheally intubated and mechanically ventilated. Bleomycin (5 U per kg body weight) or 0.9% saline was then intratracheally instilled using a microsprayer. After 24 h, mice received an intraperitoneal injection of 0.5 mg TSA per kg body weight or 0.9% saline which was repeated daily for 3 subsequent days. At the conclusion of the experiment, mice were sacrificed with 500 mg pentobarbital per kg body weight.

3.2.9.2. Lung tissue collection and weight measurements

After the thoracic cavity was exposed, lungs were perfused with 1× PBS injected *via* the right ventricle. The trachea was then dissected and lung was removed. The right lung was snap-frozen in liquid nitrogen and subjected to RNA isolation and gene expression analysis as described above. The left lobe was used to assess the lung wet-to-dry weight ratio by the gravimetric method. After the wet lung weight was measured, the lung was incubated at 60 °C for 72 h in an oven. Then, the dry lung weight was measured and ratio between wet and dry left lung weights was calculated.

3.2.9.3. Broncho-alveolar lavage

The lung and trachea were exposed as described above. After the lung was cannulated *via* the trachea, the left main bronchus was clamped and the right lung was lavaged three times with 300 µl 0.9% NaCl. The clamp was then removed, attached to the right main bronchus, and the lavage was collected from the left lung. The BAL fluid was collected after each wash and pooled. Subsequently, BAL fluid was centrifuged at 1780 rpm for 10 min at 4 °C. The supernatant and cell pellet were collected separately and used for protein concentration measurements and analyses of inflammatory cell populations, respectively.

3.2.9.4. Measurement of protein concentration in broncho-alveolar lavage fluid

To measure protein concentration, 10 µl BAL fluid supernatant, 0.9% NaCl and bovine serum albumin protein standard were transferred into a 96-well plate. Next, 200 µl of Pierce® BCA protein assay reagent was added to each well, plate was incubated at 37 °C for 30 min and absorbance was measured at 562 nm wavelength using a VersaMax micro-plate reader. Protein concentrations in BAL fluid were calculated for each sample using a standard curve.

3.2.9.5. Analysis of inflammatory cell populations

The cell pellet formed after BAL fluid centrifugation was resuspended in 1 ml of 0.9% NaCl. Subsequently, 100 µl of cell suspension was loaded onto assembled CellSpin preparation system and centrifuged at 500 rpm for 5 min. Slides were then dried and cells were stained with May-Grünwald solution for 5 min followed by incubation in Giemsa solution diluted 1:10 in water for 10 min. The differential cell count of alveolar macrophages, neutrophils and lymphocytes was then made under a light microscope and expressed as a percentage of the total cell population in the BAL fluid.

3.2.9.6. Evans blue extravasation assay

Evans blue dye (20 mg per kg body of weight) was injected into the tail vein 3 h before mice were sacrificed. At the time of killing, 1 ml of blood was collected by cardiac puncture, centrifuged at 1300 rpm for 10 min at RT and the blood plasma was diluted in formamide 1:100. The lung was perfused with PBS *via* the right ventricle, homogenized in a Precellys® 24 homogenizer and diluted in two volumes of formamide. Blood plasma and lung homogenate samples diluted in formamide were then incubated at 60 °C for 16 h to extract the Evans blue dye. Subsequently, the lung homogenate was centrifuged at 5000 g for 30 min at RT and the pellet was discarded. The absorbance of Evans blue in blood plasma and lung homogenate was then measured at 620 nm and corrected for the presence of heme by absorbance measurements at 740 nm. The corrected Evans blue absorption was then calculated as follows $A_{620\ (corrected)} = A_{620} - (1.426 \times A_{740} + 0.03)$ for lung homogenates and blood plasma. The Evans blue index reflecting the microvascular permeability of the dye was expressed as ratio of $A_{620\ (corrected)}$ in the lung homogenate to the $A_{620\ (corrected)}$ in the blood plasma.

3.3. Statistical analyses

Values are presented as mean ± SEM. Statistical comparisons between means of two groups were performed using unpaired Student's *t*-tests. For multiple comparisons, statistical analysis was performed using one-way ANOVA followed by a Tukey's *post-hoc* test. *P*-values less than 0.05 were considered significant.

4. Results

4.1. Pulmonary expression of genes encoding Na,K-ATPase subunits in lungs from acute respiratory distress syndrome patients and in healthy lung tissue

The expression of the *ATP1A1*, *ATP1B1* and *FXYD1-FXYD7* genes encoding Na,K-ATPase subunits in lung tissue from patients with ARDS was analyzed by qPCR. The expression of genes in lung homogenates was compared between four donors and five ARDS patients. The downregulation of *ATP1B1* gene expression was noted in samples from ARDS patients when compared to apparently healthy lung donors as depicted in Figure 6. Moreover, the expression of the *FXYD1* and *FXYD3* genes was significantly upregulated in ARDS patients, while *ATP1A1*, *FXYD2* and *FXYD4-FXYD7* gene expression remained unchanged comparing the two sample groups.

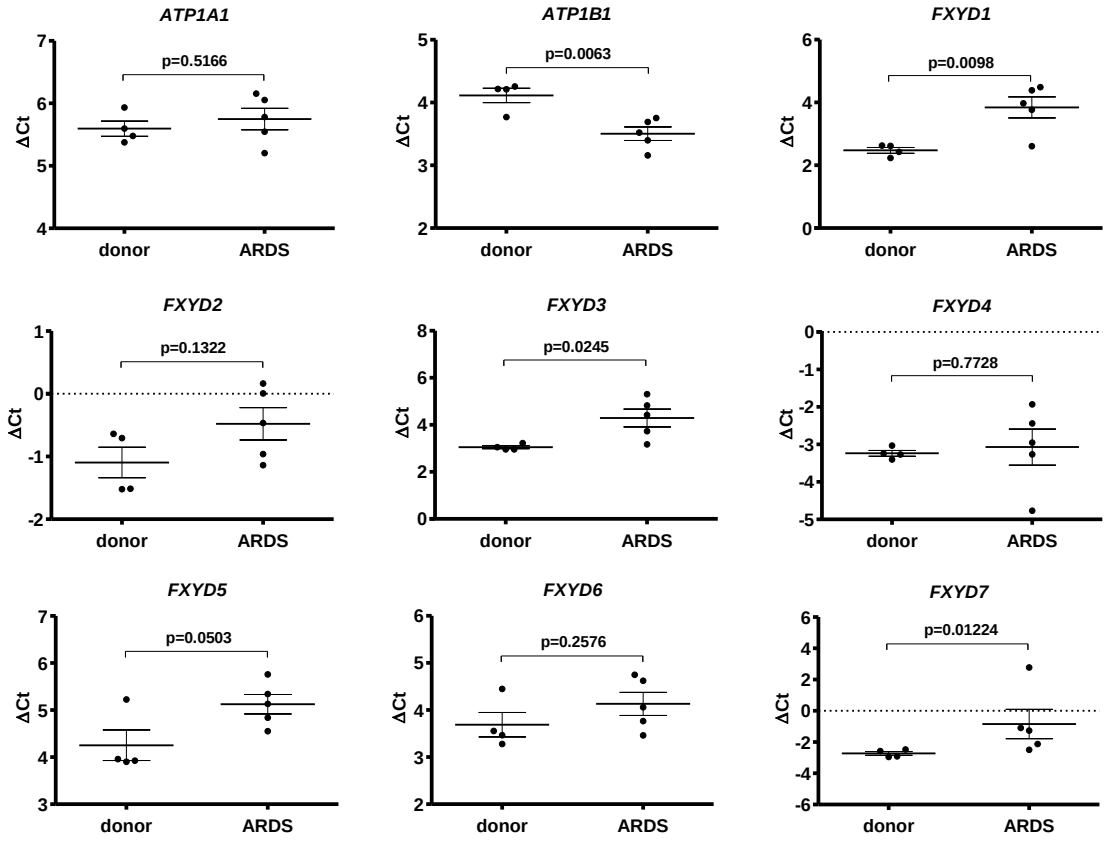

Figure 6. Pulmonary expression of genes encoding Na,K-ATPase subunits in donor *versus* ARDS patients. The expression of the *ATP1A1*, *ATP1B1* and *FXYD1-FXYD7* genes was assessed in lung tissue from five patients with ARDS or four healthy lung donors by qPCR. Data are expressed as mean ± SEM.

4.2. TGF-β alters the expression of genes encoding Na,K-ATPase subunits in A549 cells

The A549 cell-line is frequently used as a model for the human alveolar epithelium. In order to verify whether TGF-β has a regulatory role governing the expression of genes encoding Na,K-ATPase subunits in an epithelial-like cell-line, qPCR analysis was performed. Figure 7 depicts the diverse effect of TGF-β on the expression of Na,K-ATPase subunits encoding genes.

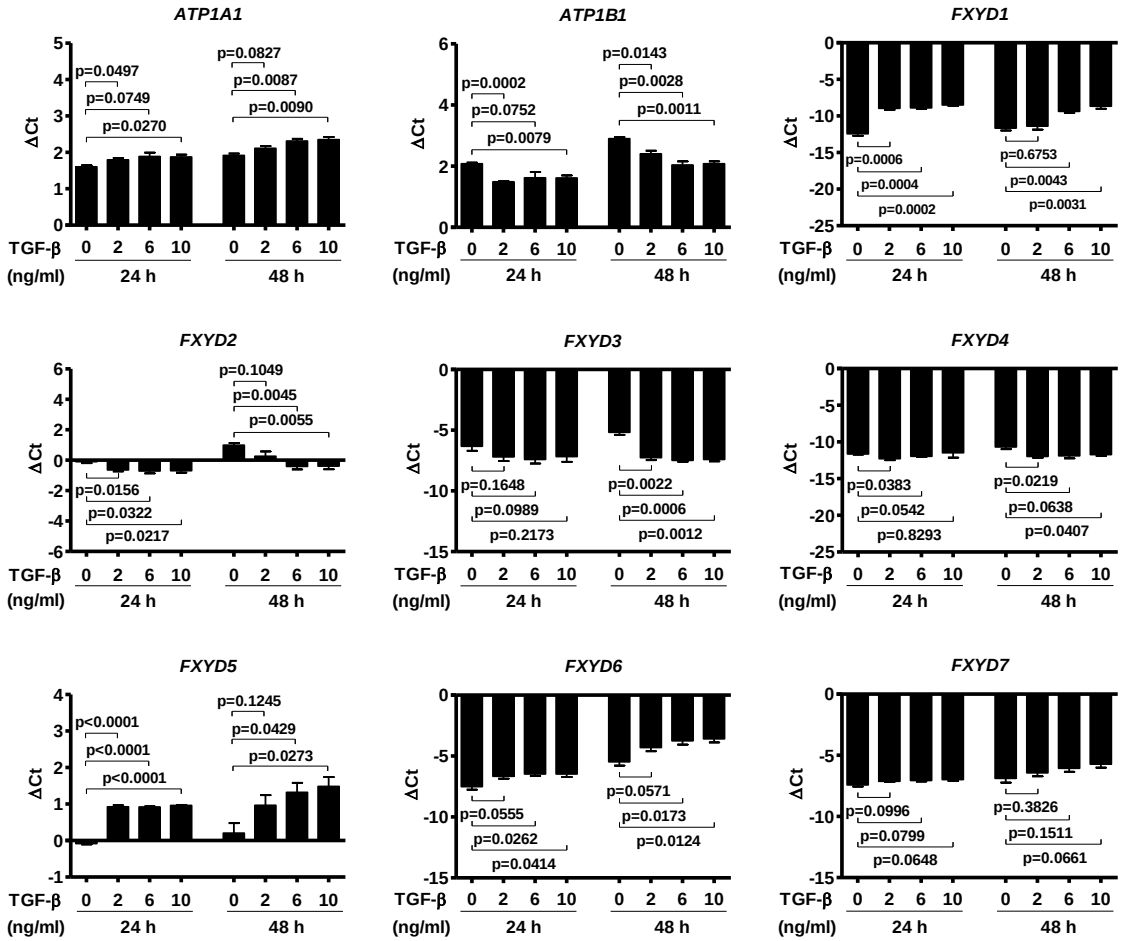

Figure 7. Expression of genes encoding Na,K-ATPase subunits in TGF-β-treated A549 cells. The expression of the *ATP1A1*, *ATP1B1* and *FXYD1-FXYD7* genes was assessed in the A549 cells stimulated with 0-10 ng/ml of TGF-β1 for 24 h or 48 h by qPCR (*n*=3, per group). Data are expressed as mean ± SEM.

The TGF-β treatment induced expression of *ATP1A1*, *FXYD1*, *FXYD5* and *FXYD6* genes and decreased the expression of *ATP1B1*, *FXYD2*, *FXYD3* and *FXYD4* genes. The expression of *FXYD7* remained unaffected. Furthermore, the effect of TGF-β on *FXYD3* mRNA abundance was time-dependent as only TGF-β treatment for 48 h but not 24 h caused repression of this gene. Additionally, genes *ATP1A1*, *FXYD1*, *FXYD2*, *FXYD5* and *FXYD6* were dose-dependently regulated by TGF-β.

4.3. Inhibition of TGF-β signaling restores *ATP1B1* gene expression

TGF-β utilizes SMAD2 and SMAD3 transcription factors as primary mediators of the TGF-β-regulated gene expression program. To test whether SMAD2 and SMAD3 were implicated in regulation of the *ATP1B1* gene, A549 cells were pre-treated with SB431542, a selective inhibitor of the TBRI receptors, ALK4, ALK5 and ALK7, and then stimulated with TGF-β. As demonstrated in Figure 8A and 8B, treatment with SB431542 drastically reduced phosphorylation of the SMAD2 and SMAD3 in the TGF-β-treated cells. Furthermore, SB431542 prevented repression of the *ATP1B1* gene indicating that TGF-β signaling employs R-SMADs to regulate expression of the *ATP1B1* gene (Figure 8C).

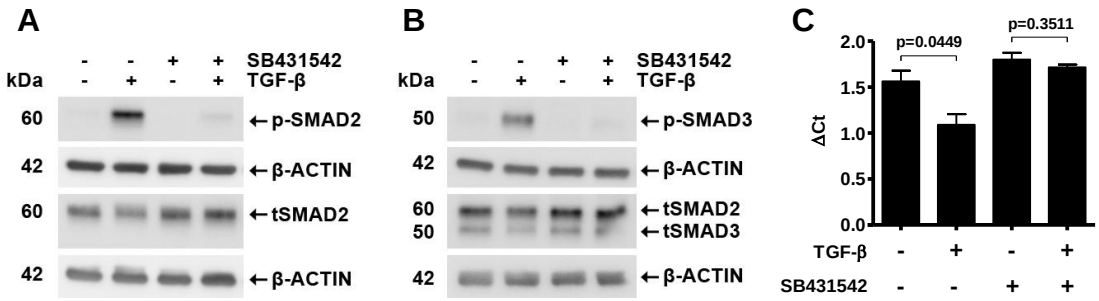

Figure 8. Inhibition of the TGF-β type I receptor alleviates *ATP1B1* gene repression by TGF-β. The impact of SB431542 on the phosphorylation of SMAD2 (A) and SMAD3 (B). The A549 cells were first treated with 20 μM SB431542 for 1 h followed by stimulation with 10 ng/ml TGF-β1 for 1 h. Total cellular proteins were isolated, subjected to western blot and immunohistochemically stained with antibodies against phosphorylated SMAD2, phosphorylated SMAD3, total SMAD2, total SMAD2/SMAD3 and β-ACTIN. (C) Expression analysis of the *ATP1B1* gene was assessed in A549 cells stimulated with 0 ng/ml or 10 ng/ml of TGF-β1 for 48 h, by qPCR. The 20 μM SB431542 was added 1 h before the TGF-β1 stimulation for 49 h (*n*=3, per group). Data are expressed as mean ± SEM.

4.4. TGF-β downregulates *ATP1B1* gene expression *via* SMAD2, SMAD4, SNAI1 and E2F5 transcription factors

TGF-β signaling is a complex process involving the activity of many different transcription factors in order to achieve precise regulation of target gene expression. In order to characterize the transcription factors involved in the TGF-β-dependent down-regulation of the *ATP1B1* gene, a series of knock-down experiments was performed. Lipofectamine™ 2000-mediated delivery of siRNA molecules designed against TGF-β signaling-associated transcription factors was selected to take advantage of the relatively efficient transfection rates of A549 cells using cationic lipid formulations. At the 24 h or 48 h time-point before TGF-β stimulation, A549 cells were transfected with 100 nM or 200 nM siRNA targeting the SMAD2, SMAD3, SMAD4, YY1, RUNX2, TGIF, SNON, SNAI1, E2F4 and E2F5 transcription factors, which led to a marked decrease in protein abundance as demonstrated by western blot (Figure 9).

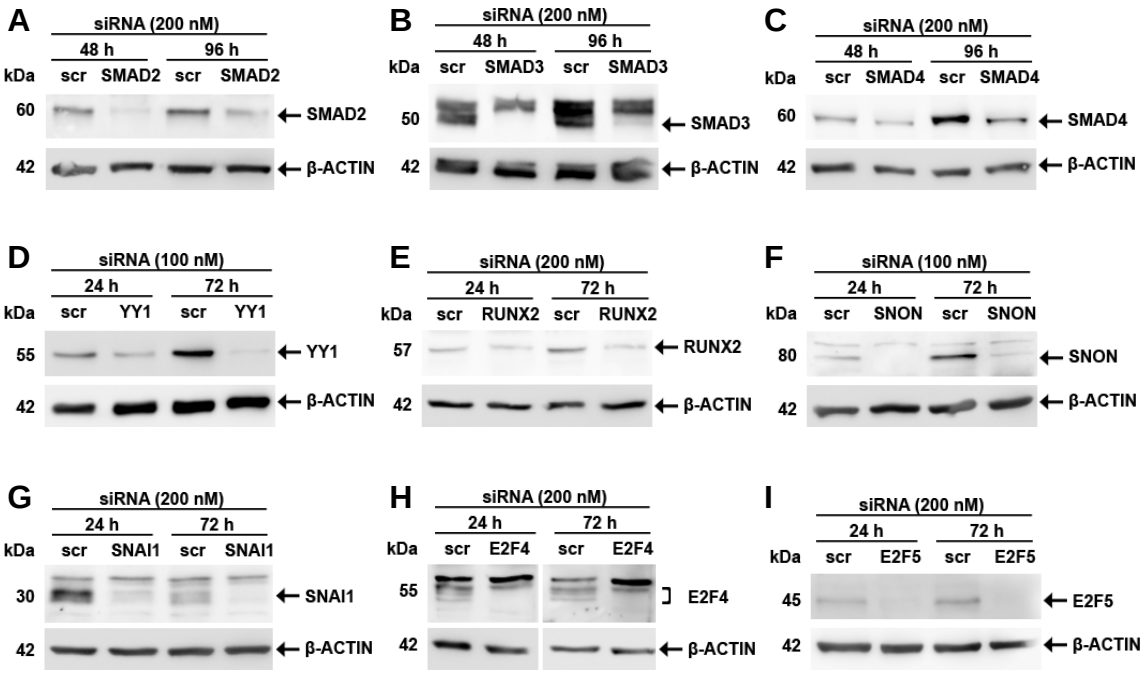

Figure 9. Optimization of siRNA knock-down of transcription factors involved in TGF-β signaling. The A549 cells were transfected with 100 nM or 200 nM of scrambled (scr) siRNA or siRNA designed against SMAD2 (A), SMAD3 (B), SMAD4 (C), YY1 (D), RUNX2 (E), SNON (F), SNAI1 (G), E2F4 (H) or E2F5 (I) for 24 h and 72 h or 48 h and 96 h. A western blot was used to confirm the knock-down of transcription factor proteins.

An analysis of *ATP1B1* gene expression by qPCR revealed that the depletion of SMAD3, YY1, RUNX2, TGIF, SNON and E2F4 transcription factors did not impact the ability of TGF-β to down-regulate the *ATP1B1* gene expression (Figure 10B, 10D-F and 10H). However, the *ATP1B1* gene was relieved from repression by TGF-β in cells where SMAD2, SMAD4, SNAI1 or E2F5 were depleted by knock-down (Figure 10A, 10C, 10G and 10I). These data indicate that SMAD2, SMAD4, SNAI1 and E2F4 mediate the downregulation of *ATP1B1* gene expression by TGF-β.

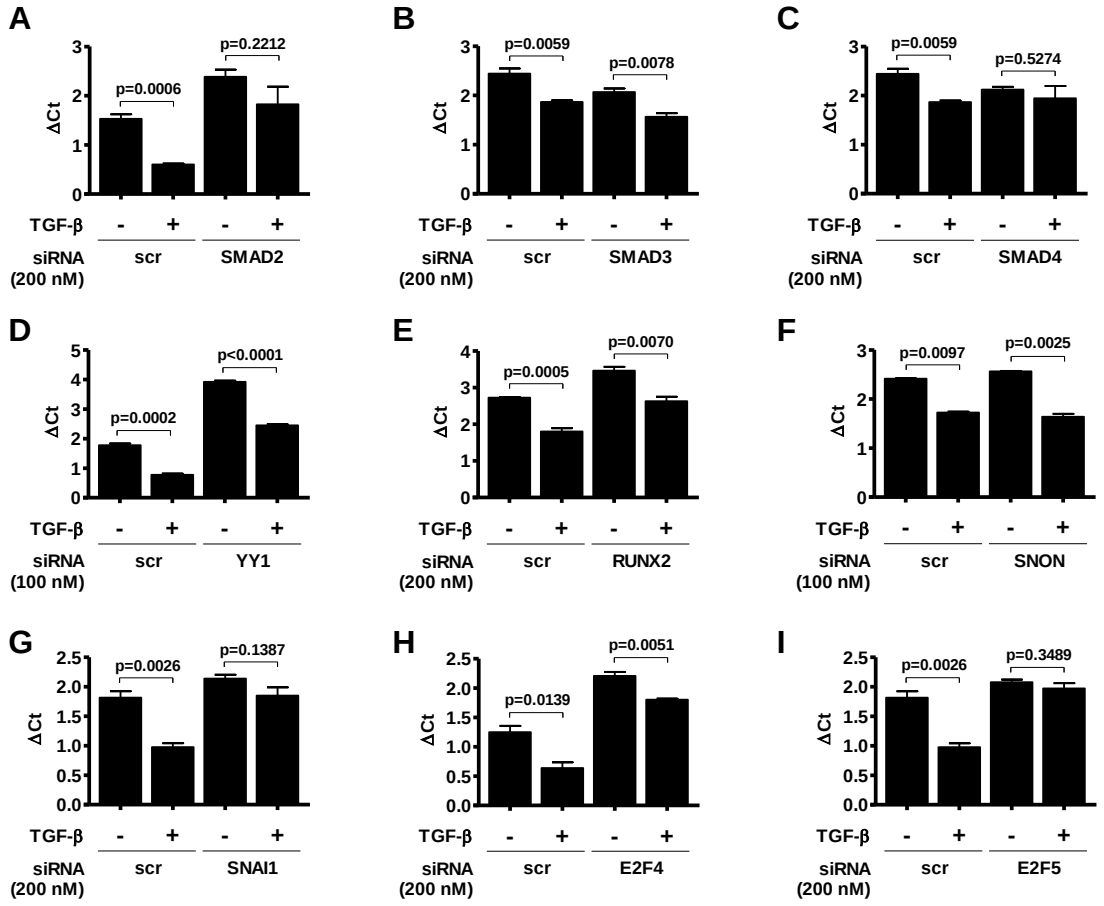

Figure 10. Regulation of the *ATP1B1* gene by TGF-β signaling-associated transcription factors. Expression of the *ATP1B1* gene in A549 cells with knock-down of SMAD2 (A), SMAD3 (B), SMAD4 (C), YY1 (D), RUNX2 (E), SNON (F), SNAI1 (G), E2F4 (H) or E2F5 (I) transcription factors. The A549 cells were transfected with 100 nM or 200 nM of siRNA. At 24 h or 48 h later, 10 ng/ml of TGF-β1 was added to transfection medium for additional 48 h. The expression of *ATP1B1* gene was then analyzed by qPCR (n=3, per group). Data are expressed as mean ± SEM.

4.5. TGF-β downregulates *ATP1B1* promoter activity

To confirm that TGF-β signaling controls the expression of the *ATP1B1* gene at the level of gene transcription, the 1837-bp DNA fragment spanning the upstream region the *ATP1B1* gene (-3075 to -1238 bp upstream from transcription start site) was cloned into pGL3-Basic vector. The activity of the *ATP1B1* promoter was measured by a dual-luciferase reporter assay. TGF-β significantly decreased the activity of *ATP1B1* promoter (Figure 11A) revealing that TGF-β inhibits the expression of the *ATP1B1* gene on the transcription level.

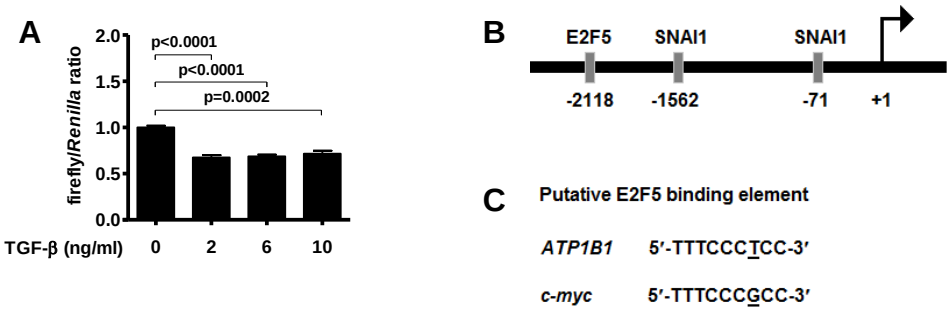

Figure 11. The *ATP1B1* promoter analysis in A549 cells treated with TGF-β. (A) A dual-luciferase reporter assay of *ATP1B1* gene promoter activity. Cells were transiently co-transfected with a pGL3-Basic-*ATP1B1*-promoter firefly luciferase reporter plasmid and pRL-SV40 *Renilla* luciferase co-reporter vector and were then stimulated with 0-10 ng/ml TGF-β1 for 48 h (*n*=4, per group). Data are expressed as mean ± SEM. (B) Schematic representation of 3 kbp region of the *ATP1B1* promoter. Novel putative bindings sites for E2F5 (-2118 bp) and SNAI1 (-1562 bp) along previously characterized SNAI1 binding site (-71 bp) are shown. (C) Sequence comparison of the E2F5 binding element from *c-myc* promoter to putative E2F5 binding site in the *ATP1B1* promoter. Differing nucleotides are underlined.

Sequence analysis of the promoter region spanning 3000 bp upstream from the transcriptional start site revealed the presence of putative binding sites for SNAI1 and E2F5 transcription factors. The noncanonical E-box element, a SNAI1-binding sequence, located within -71 to -66 bp upstream from transcription start site was previously characterized (Espineda *et al.*, 2004). Analysis of the further upstream regions of the promoter uncovered a site identical in sequence to the E-box element (5′-CCGGTG-3′) characterized by Espineda *et al.* albeit -1562 to -1557 bp upstream from the transcriptional start site (Figure 11B). Additionally, a site highly similar

to the E2F5-binding element reported by Chen and coworkers was located at -2118 to -2110 bp (Figure 11C). The putative E2F5 binding site localized in the *ATP1B1* gene promoter varied from the TGF-β responsive element described in the *c-myc* promoter by the presence of the single thymine base instead of the guanine at position seven of the sequence (Chen *et al.*, 2002).

4.6. The TGF-β-dependent down-regulation of *ATP1B1* gene expression is mediated by DNA methylation and class I histone deacetylases

To test whether inhibition of *ATP1B1* expression by TGF-β involves the action of the epigenetic machinery, 5-Aza-2′-dC and TSA were employed to inhibit DNA methylation and histone deacetylation, respectively. Prevention of DNA methylation by 5-Aza-2′-dC abolished TGF-β-triggered downregulation of the *ATP1B1* gene expression as assessed by qPCR (Figure 12A). Additionally, the influence of DNA methylation on the *ATP1B1* promoter was tested. The treatment with 5-Aza-2′-dC alone reduced the activity of the *ATP1B1* promoter to the level observed under the TGF-β conditions. Moreover, TGF-β did not further reduce the activity of the *ATP1B1* promoter in A549 cells co-treated with 5-Aza-2′-dC (Figure 12B).

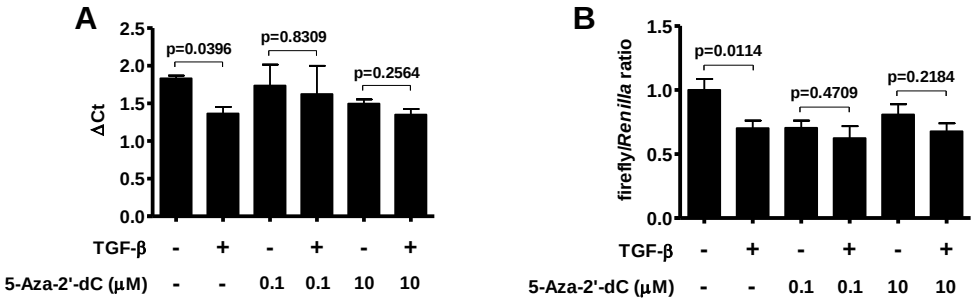

Figure 12. Activity of the *ATP1B1* gene and promoter is regulated by DNA methylation. (A) Analysis of *ATP1B1* gene expression in A549 cells stimulated with 0 ng/ml or 10 ng/ml of TGF-β1 for 48 h by qPCR (*n*=3, per group). 24 h before TGF-β1 treatment and at the 0 h and 24 h time-points after TGF-β1 stimulation, 0, 0.1 or 10 μM 5-Aza-2′deoxycytidine (5-Aza-2′-dC) was added. (B) A dual-luciferase reporter assay of the *ATP1B1* promoter activity (*n*=9, per group). Cells were stimulated with TGF-β1 or 5-Aza-2′-dC as in (A). Data are expressed as mean ± SEM.

To test whether TGF-β signaling recruits HDACs to repress the *ATP1B1* gene, the pan-HDAC inhibitor, TSA, was used. Histone deacetylase inhibition abrogated the repression of the *ATP1B1* gene by TGF-β (Figure 13A). Moreover, the involvement of HDACs in the repression was further confirmed by evidence of decreased *ATP1B1* promoter activity in the TGF-β stimulated cells co-treated with TSA (Figure 13C). To characterize the nature of the complexes repressing the *ATP1B1* gene, class-specific inhibitors of HDAC enzymes were employed. The TGF-β-induced repression of the *ATP1B1* gene was specifically facilitated by class I HDAC enzymes, since use of the class I HDAC inhibitor MGCD0103 but not MC1568 (a class II HDAC inhibitor) removed the TGF-β effect (Figure 13B). Moreover, the involvement of class I HDAC has been verified by promoter activity assay, where MGCD0103 alleviated the response to TGF-β, while use of the class II HDAC inhibitor did not repeat this result (Figure 13C).

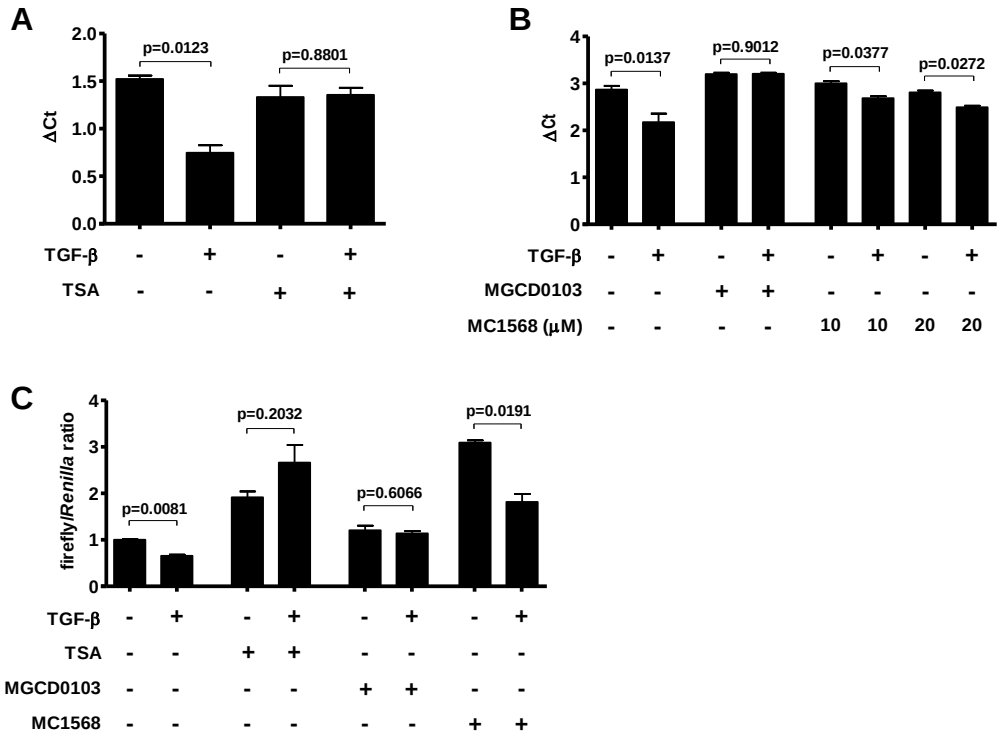

Figure 13. Class I histone deacetylases regulate *ATP1B1* gene expression and promoter activity. (A), (B) and (C) The A549 cells were stimulated with 0 ng/ml or 10 ng/ml of TGF-β1 for 48 h. At 24 h after TGF-β1 was added, 64 nM pan-HDAC inhibitor trichostatin A (TSA), 10 μM (C) class I or class II HDAC inhibitors (MGCD0103 or MC1568, respectively) were added for 24 h (*n*=3-4, per group). (A) and (B) Expression of the *ATP1B1* was assessed by qPCR. (C) A dual-luciferase reporter assay of the *ATP1B1* promoter activity (*n*=3, per group). Data are expressed as mean ± SEM.

4.7. Histone deacetylase 2 mediates repression of the *ATP1B1* gene by TGF-β

To characterize which member of the class I HDACs repress *ATP1B1* gene expression after TGF-β stimulation, the siRNA approach was employed to knock-down HDAC1, HDAC2 and HDAC3 proteins. As demonstrated in Figure 14A-C, the control western blot confirmed that siRNA transfections decreased the abundance of HDAC1, HDAC2 and HDAC3 proteins. The knock-down of the HDAC2 expression by siRNA resulted in a diminished effect of TGF-β on *ATP1B1* gene expression (Figure 14E). This effect was specific only to cells displaying HDAC2 knock-down, since depletion of HDAC1 or HDAC3 did not impact *ATP1B1* gene repression (Figure 14D and 14F).

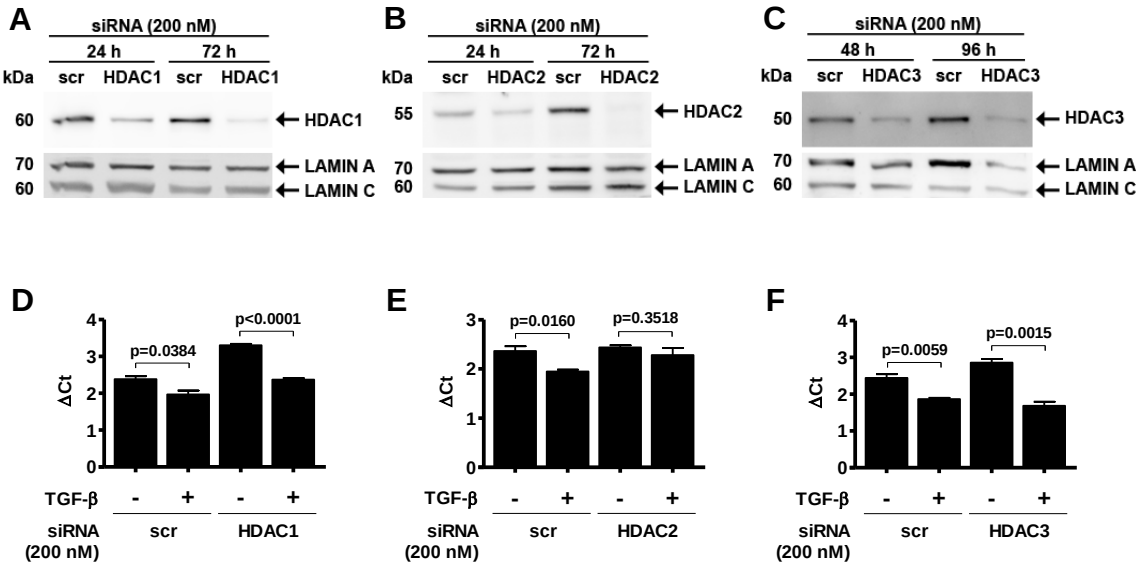

Figure 14. A particular role for histone deacetylase 2 in the regulation of *ATP1B1* gene repression. Optimization of siRNA knock-down of HDAC1 (A), HDAC2 (B) or HDAC3 (C) transcription co-factors. The A549 cells were transfected with 200 nM of scrambled (scr) siRNA or siRNA designed against one of the HDAC-encoding mRNA for 24 and 72 or 48 and 96 h. A western blot was used to confirm knock-down of HDAC protein. Expression of the *ATP1B1* gene in A549 cells with knock-down of HDAC1 (D), HDAC2 (E) or HDAC3 (F) proteins. The A549 cells were transfected with 200 nM of siRNA. At 24 or 48 h later, 10 ng/ml of TGF-β1 was added to transfection medium for additional 48 h. The expression of the *ATP1B1* gene was then analyzed by qPCR (*n*=3, per group). Data are xpressed as mean ± SEM.

4.8. Histone deacetylase 2 occupies the *ATP1B1* promoter and is activated by TGF-β

To investigate whether HDAC2 can be located in the *ATP1B1* gene promoter a ChIP technique was employed. In principle, the ChIP assay allows for the detection of a specific DNA sequence which interacts with immunoprecipitated proteins of interest. As a transcriptional co-repressor, HDAC2 does not bind DNA directly, and is not located in close proximity to DNA, which limits the effectiveness of the short-arm cross-linker formaldehyde that is commonly used in the ChIP assay. In the present study, the DNA-protein cross-linking procedure was modified by the introduction of the long-arm cross-linker DSP to capture the weak association between HDAC2 and DNA. Immunoprecipitation of the HDAC2 was confirmed by western blot by identification of a band migrating with a molecular mass of 55 kDa (Figure 15A). As a 55 kDa band was not detected when an isotype control antibody was used instead of an anti-HDAC2 antibody, the specificity of the HDAC2 immunoprecipitation was confirmed. Analysis of DNA cross-linked to HDAC2 by PCR resulted in amplification of *ATP1B1* promoter region located -1339 to -1241 bp upstream from the transcriptional start site (Figure 15B). The TGF-β treatment for 3 h did not impact the intensity of the -1339 to -1241 bp amplicon, suggesting that TGF-β does not increase *ATP1B1* promoter occupancy by HDAC2. The absence of DNA amplification when an isotype control antibody was used confirmed the specificity of the ChIP. To further test the specificity of the ChIP assay, exon three of the reference gene *HPRT1* was chosen to represent a region potentially uninvolved in transcriptional regulation and HDAC2 binding. No DNA amplification was observed when semiquantitative PCR with primers recognizing exon three in *HPRT1* gene was performed on chromatin immunoprecipitated with an anti-HDAC2 or isotype control antibody (Figure 15C). These data suggest that immunoprecipitates were not contaminated with DNA fragments which were not bound to HDAC2. To obtain quantitative data for TGF-β impact on the sequestration of the HDAC2 to the *ATP1B1* promoter, a qPCR technique was employed. As illustrated in Figure 15D, TGF-β treatment did not significantly induce the accumulation of HDAC2 in region -1339 to -1241 bp of the *ATP1B1* promoter, thereby confirming that TGF-β does not increase the occupancy of HDAC2 on the *ATP1B1* promoter.

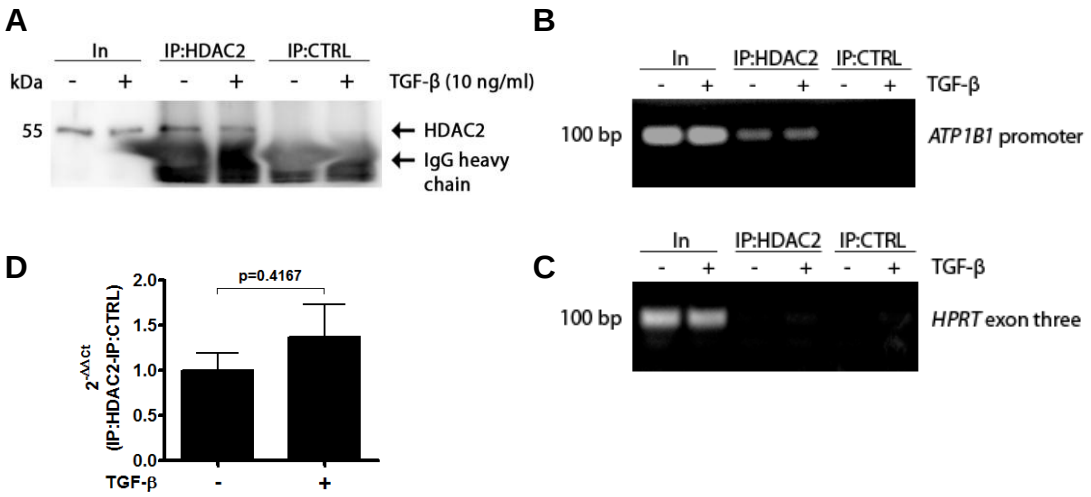

Figure 15. Histone deacetylase 2 occupancy of the *ATP1B1* promoter. (A) Control western blot confirming specific immunopreciopitation of HDAC2. (B), (C) and (D) ChIP assay of the HDAC2 enrichment in the *ATP1B1* promoter region located -1339 to -1241 bp upstream from transcriptional start site in A549 cells stimulated with 0 or 10 ng/ml TGF-β1 for 3 h. (B) PCR amplification of the *ATP1B1* promoter. (C) PCR amplification of exon three of the *HPRT1* gene. (D) Fold-change of the relative *ATP1B1* promoter DNA abundance assessed by qPCR. IgG, Immunglobulin G; In, Input; IP:HDAC2, immunoprecipitation with anti-HDAC2 antibody; IP:CTRL, immunoprecipitation with isotype-matched nonspecific antibody (*n*=3, per group).

Since TGF-β treatment did not increase enrichment of HDAC2 at the *ATP1B1* promoter site, the possibility that TGF-β signaling can regulate HDAC2 activity was investigated. The phosphorylation of HDAC2 at serine 394 has been linked to increased enzymatic activity and speculated to be an important step allowing the formation of repressor complexes (Tsai and Seto, 2002). Therefore, the impact of TGF-β on the phosphorylation at serine 394 of HDAC2 was evaluated by western blot. As depicted in Figure 16, treatment with TGF-β increased phosphorylation of serine 394 which was observed over 3 h time course after stimulation indicating that TGF-β signaling can activate HDAC2.

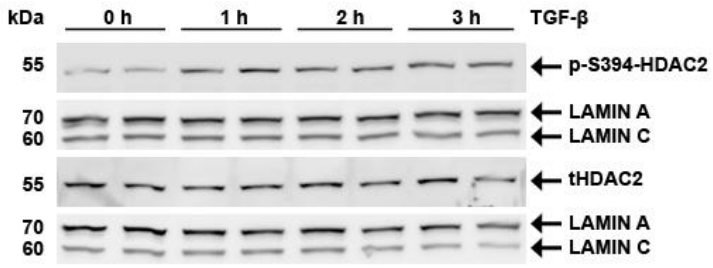

Figure 16. Impact of TGF-β on the phosphorylation status of HDAC2. The A549 cells were stimulated with 0 ng/ml or 10 ng/ml of TGF-β1 for 1, 2 or 3 h. Total cellular proteins were isolated, subjected to western blot and immunochemically stained with antibodies against HDAC2 phosphorylated at serine 394, total HDAC2 and LAMIN A/C (*n*=4, per group).

4.9. Downregulation of the *Atp1b1* gene in TGF-β-stimulated alveolar epithelial type II cells can be reversed by inhibition of class I histone deacetylases

Isolated primary mouse AETII cells were used to verify whether TGF-β regulates *Atp1b1* gene expression in epithelial cells in primary culture. As demonstrated in Figure 17, treatment with TGF-β for 48 h resulted in repression of the *Atp1b1* gene in primary AETII cells cultured under air-liquid conditions.

To test whether HDAC proteins mediate regulation of the *Atp1b1* gene by TGF-β, the pan-HDAC inhibitor TSA was employed. The TGF-β stimulation increased the expression of the *Atp1b1* gene in TSA-treated AETII cells (Figure 17). The MGCD0103 and MC1568 inhibitors were used to discriminate which class of HDAC enzymes was involved in the regulation of the *Atp1b1* gene by TGF-β in mouse AETII cells. The *Atp1b1* gene was released from the TGF-β-controlled repression exclusively in AETII cells co-treated with MGCD0103 (class I HDAC inhibitor). Conversely, use of the class II HDAC inhibitor, MC1568, did not influence the TGF-β-induced repression of the *Atp1b1* gene (Figure 17). These data confirm a key role for class I HDACs in the repression of the *ATP1B1* gene by TGF-β in alveolar epithelial cells.

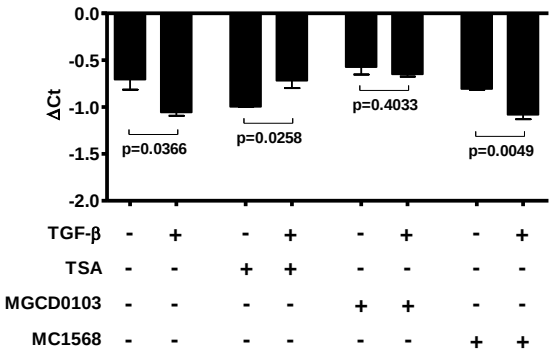

Figure 17. Regulation of *Atp1b1* gene expression in alveolar epithelial type II cells by TGF-β and class I histone deacetylases. Analysis of *Atp1b1* gene expression in primary mouse alveolar epithelial type II cells stimulated with 0 ng/ml or 10 ng/ml of TGF-β1 for 48 h by quantitative PCR. At 24 h after TGF-β1 stimulation, 64 nM pan-HDAC inhibitor trichostatin A (TSA), 10 μM class I or class II HDAC inhibitors (MGCD0103 or MC1568, respectively) were added for 24 h (*n*=3, per group). Data are expressed as mean ± SEM.

4.10. Histone deacetylase inhibition rescues *Atp1b1* gene expression and decreases lung water content in the bleomycin model of acute respiratory distress syndrome

Several groups have reported TGF-β signaling to be deregulated and to mediate ARDS in human patients and lung injury in various animal models of ARDS (Budinger *et al.*, 2005, Wesselkamper *et al.*, 2005, Dhainaut *et al.*, 2003, Fahy *et al.*, 2003, Pittet *et al.*, 2001). Here, TGF-β signaling has been reported to employ HDAC2 to downregulate *ATP1B1* gene expression in A549 cells which could be alleviated by HDAC2 inhibition. Moreover, *Atp1b1* gene expression was downregulated in primary mouse AETII cells treated with TGF-β, and this effect was alleviated by HDAC inhibition. Therefore, the impact of the pan-HDAC inhibitor TSA on the expression of the *Atp1b1* gene in bleomycin model of ARDS has been investigated. Expression of the *Atp1b1* gene in murine lungs five days post-bleomycin instillation was reduced (Figure 18A) while lung water content was increased (Figure 18B). Remarkably, administration of the TSA to bleomycin-instilled mice restored the expression of the *Atp1b1* gene (Figure 18A). Moreover, increased *Atp1b1* gene expression by TSA was accompanied by decreased lung water (Figure 18B) when compared to bleomycin-only treated mice. Based on these

data, it can be concluded that histone deacetylases mediate the repression of the *Atp1b1* gene *in vivo* and are involved in modulation of pulmonary edema.

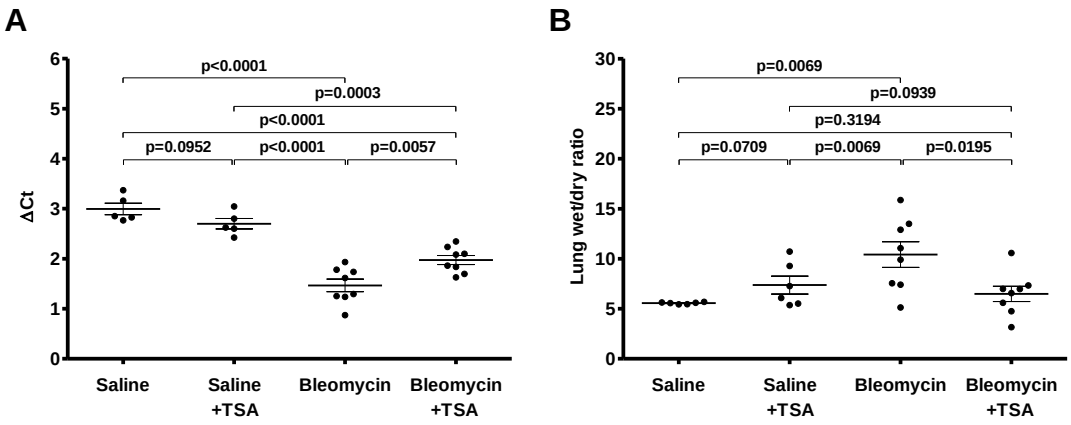

Figure 18. Effect of trichostatin A on *Atp1b1* gene expression and pulmonary edema in the bleomycin model of acute respiratory distress syndrome. C57BL/6J mice were instilled with bleomycin to initiate lung injury. At 24 h later, mice received intraperitoneal injection of trichostatin A (TSA) or vehicle for four subsequent days. After animals were sacrificed, RNA was isolated and *Atp1b1* gene expression was analyzed by qPCR (A) and lung edema level was evaluated by the gravimetric method and expressed as lung wet-to-dry ratio (B). Data are expressed as mean ± SEM (*n*=5-8, per group).

4.11. Trichostation A does not decrease alveolar-capillary barrier permeability in bleomycin-treated mice

The impact of the TSA on alveolar-capillary barrier function in the bleomycin ARDS model was assessed by measurement of the total protein concentration in the BAL fluid and by Evans blue extravasation assay. As depicted in Figure 19A and 19B, bleomycin instillation induced the accumulation of protein in the BAL fluid and increased permeability of the endothelial barrier to Evans blue dye. However, TSA treatment did not decrease total protein levels in BAL fluid and did not reduce the Evans blue index. These data indicate that TSA does not affect permeability of the alveolar-capillary barrier in the bleomycin model of ARDS.

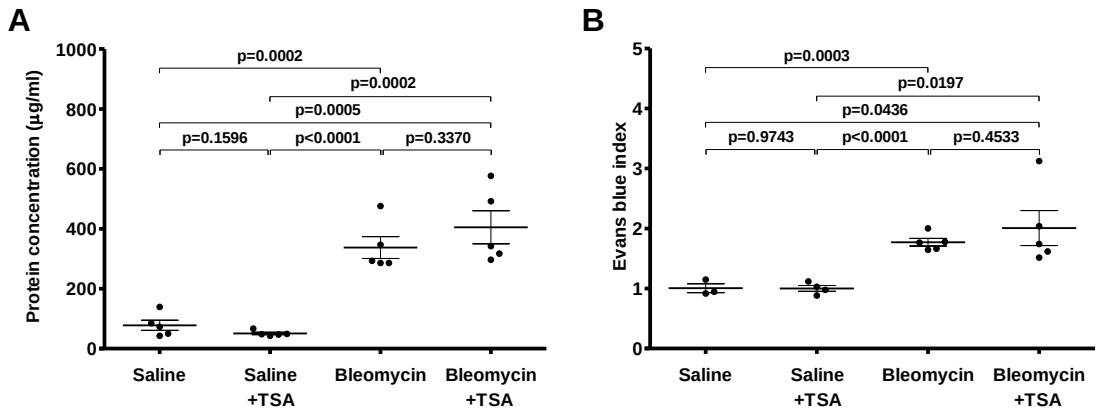

Figure 19. Effect of trichostatin A on alveolar-capillary barrier permeability in the bleomycin model of acute respiratory distress syndrome. C57BL/6J mice were instilled with bleomycin to initiate lung injury. At 24 h later, mice received intraperitoneal injection of trichostatin A (TSA) or vehicle for four subsequent days. The alveolar-capillary barrier permeability was analyzed by measurement of the total protein concentration in the broncho-alveolar lavage fluid (A) and Evans blue extravasation assay (B). Data are expressed as mean ± SEM (*n*=3-5, per group).

4.12. The inflammatory response is not modified by histone deacetylase inhibition in the bleomycin model of acute respiratory distress syndrome

Alveolar macrophages, neutrophils and lymphocytes mediate the inflammatory response in ARDS. The differential analysis of the inflammatory cells in BAL fluid revealed that bleomycin instillation decrease the number of alveolar macrophages and promoted neutrophil and lymphocyte recruitment to the lung in bleomycin model of ARDS (Figure 20). However, the treatment with TSA did not increase the percentage of alveolar macrophages (Figure 20A) and did not reverse neutrophil and lymphocyte sequestration to the alveoli after bleomycin instillation (Figure 20B and 20C). These data indicate that histone deacetylases do not mediate inflammatory responses in the bleomycin model of ARDS.

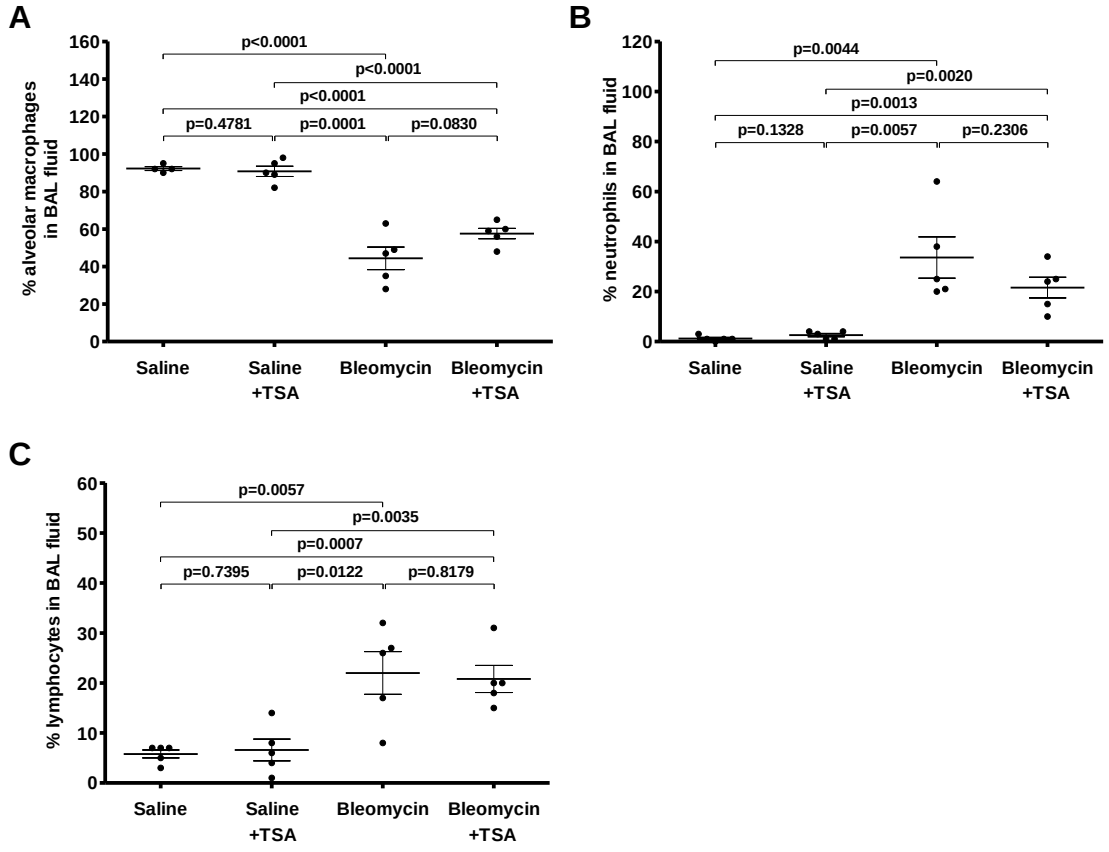

Figure 20. The effect of trichostatin A on inflammatory responses in the bleomycin model of acute respiratory distress syndrome. C57BL/6J mice were instilled with bleomycin to initiate lung injury. 24 h later, mice received an intraperitoneal injection of trichostatin A (TSA) or vehicle for four subsequent days. After animals were sacrificed, the BAL fluid was collected and cells were recovered by cytospin centrifugation. Mean % of alveolar macrophages (A), neutrophils (B) and lymphocytes (C) in BAL fluid was identified by differential staining. Data are expressed as mean ± SEM (*n*=5, per group).

5. Discussion

The current concept of the pathological mechanisms at play in ARDS highlight the causative role of deregulated Na^+ transporting machinery which negatively impacts AFC and, therefore, promotes the persistence of pulmonary edema (Sartori and Matthay, 2002). The TGF-β is widely recognized as a critical mediator of ARDS pathogenesis, and the involvement of the TGF-β pathway in disruption of Na^+ transport and pulmonary edema formation has been established (Wesselkamper *et al*., 2005, Budinger *et al*., 2005, Fahy *et al*., 2003, Pittet *et al*., 2001). In this study, the question has been asked whether the expression of Na,K-ATPase subunit-encoding genes are differentially regulated in ARDS and if whether TGF-β can modulate expression of Na,K-ATPase subunits-encoding genes.

The comparison of *in vivo* and *in vitro* expression patterns revealed that *FXYD1* and *ATP1B1* genes were similarly regulated in lung tissues from patients with ARDS, and in TGF-β-treated A549 cells. The expression of the *FXYD1* gene was significantly upregulated in lungs from ARDS patients and in TGF-β-stimulated cells, when compared to control samples. The auxiliary subunit FXYD1 regulates Na,K-ATPase function in a tissue-specific context. The FXYD1 protein has been shown to decrease the apparent Na^+ and K^+ affinity of Na,K-ATPase (Geering, 2006). Moreover, *FXYD1*-deficient mice exhibit increased Na,K-ATPase activity in cardiomyocytes which suggests that the upregulated *FXYD1* gene expression observed in ARDS might contribute to decreased Na^+ transport across the alveolar epithelium (Geering, 2008).

The ATP1B subunit is a critical component of the Na,K-ATPase complex and ATP1B1 is the most abundantly expressed isoform in the lung (Flodby *et al*., 2012). In the present study, expression of the *ATP1B1* gene was demonstrated to be reduced in the lungs from ARDS patients and in TGF-β-treated A549 cells when compared to healthy lungs and untreated cells, respectively. A parallel trend was observed in the bleomycin model of ARDS and in primary mouse AETII cells treated with TGF-β. Furthermore, downregulation of *Atp1b1* gene expression has been also reported in a nickel model of ARDS (Wesselkamper *et al*., 2005). These data indicate that repression of the *ATP1B1* gene expression is a common reaction of the lung epithelium to injury.

5.1. The expression of the *ATP1B1* gene is strictly regulated by TGF-β

The main focus of this study was to understand the mechanism of *ATP1B1* gene repression by the TGF-β pathway. Doses of TGF-β employed in the present study (up to 10 ng/ml) were chosen to simulate pathological situation of ARDS where TGF-β was reported at a concentration of 7-14 ng/ml in BAL fluid (Budinger *et al*., 2005, Dhainaut *et al*., 2003, Fahy *et al*., 2003). The recognition of the ligand by the membrane-bound receptors marks the initiation of TGF-β signaling and immediately leads to activation of the secondary messengers, the SMAD transcription factors (Massagué and Gomis, 2006). In the present study, inhibition of the TBRI receptor by SB431542 prevented SMAD2 and SMAD3 phosphorylation, and abolished downregulation of the *ATP1B1* gene. Furthermore, specific knock-down of SMAD2 and a common partner SMAD4, but not SMAD3, rescued *ATP1B1* gene expression. Together, these results demonstrate a central role of SMAD transcription factors in *ATP1B1* gene regulation and indicate that a complex consisting of SMAD2/SMAD4 rather than SMAD3/SMAD4 mediates TGF-β-controlled repression of the *ATP1B1* gene.

Apart from SMADs, TGF-β signaling utilizes a variety of other transcription factors to control the gene expression. The siRNA-mediated knock-down of SNAI1 and E2F5, but not of YY1, RUNX2, SNON and E2F4, prevented downregulation of *ATP1B1* gene expression in response to TGF-β. Chen and colleagues investigated in the detail the interaction between SMAD2, SMAD3 and E2F5 and reported a critical role of a complex consisting of these proteins in the repression of the *c-myc* gene by TGF-β (Chen *et al*., 2002). Analysis of the *ATP1B1* promoter sequence in the present study revealed the presence of a region located at -2118 to -2110 bp upstream from transcription start site, which was highly similar to the E2F5 binding element characterized in the *c-myc* gene. The association of SNAI1 with SMAD3 and SMAD4 has been reported to play a critical role in repression of *CAR*, *OCCLUDIN*, *CLAUDIN-3* and *E-CADHERIN* genes in TGF-β-driven epithelial-to-mesenchymal transition (Vincent *et al*., 2009). More importantly, SNAI1 has been demonstrated to bind the noncanonical E-box element located in the -71 to -66 bp region upstream from the transcriptional start site of the *ATP1B1* gene, and repress this gene expression in poorly differentiated carcinoma cell lines (Espineda *et al*., 2004). However, the TGF-β-responsive *ATP1B1* promoter region (-3075 to -1238 bp) cloned for the purpose

of this study, lacked a noncanonical E-box element located within the -71 to -66 bp region upstream from the transcriptional start site. A bioinformatic analysis of the cloned *ATP1B1* promoter sequence identified another noncanonical E-box element, located in the region -1562 to -1557 bp upstream of the transcriptional start site. Since SNAI1 has been shown here to mediate TGF-β-induced repression of the *ATP1B1* gene, one can speculate that the noncanonical E-box element located within the -1562 to -1557 bp region upstream of the transcriptional start site might be alternative site recognized by SNAI1. Collectively, evidence presented here and in previously published studies indicate that SMAD2, SMAD4, SNAI1 and E2F5 are involved in *ATP1B1* gene repression by TGF-β.

5.2. TGF-β signaling employs epigenetic machinery to regulate the *ATP1B1* gene

In addition to recruitment of DNA-binding transcription factors, TGF-β signaling employs epigenetic machinery to regulate the expression of target genes (Feng and Derynck, 2005). Here, the involvement of DNA methylation in the regulation of the *ATP1B1* gene by TGF-β was investigated. The inhibition of DNA methylation by 5-Aza-2′-dC resulted in the loss of the ability of TGF-β to modulate *ATP1B1* gene transcription and promoter activity. These data suggest that TGF-β may regulate the *ATP1B1* gene by altering the DNA methylation pattern. Interestingly, the use of 10 μM 5-Aza-2′-dC reduced *ATP1B1* gene transcription and promoter activity in both TGF-β-treated as well as in control cells to the same level as in cells stimulated with TGF-β only. This observation may indicate that DNA methylation in the *ATP1B1* gene promoter is important for normal expression of this gene under normal conditions. Additionally, Thillainadesan and colleagues recently reported that TGF-β signaling recruits the DNA-demethylating machinery which has a functional impact on $p15^{ink4b}$ gene expression (Thillainadesan *et al.*, 2012). Therefore, it may be possible that TGF-β employs a DNA-demethylating complex to actively demethylate the *ATP1B1* promoter and repress the *ATP1B1* gene expression.

Regulation of histone acetylation is another epigenetic mechanism which can serve to modulate the gene expression (Wu and Grunstein, 2000). Several TGF-β associated transcription factors have been shown to recruit HDACs and to form functional complexes in order to repress target genes (Massagué *et al.*, 2005). Treatment

with the pan-HDAC inhibitor TSA released the *ATP1B1* gene from TGF-β-mediated repression in A549 cells and in primary mouse AETII cells, clearly indicating that TGF-β downregulates *ATP1B1* gene by utilizing HDACs. Furthermore, the use of class-specific HDAC inhibitors revealed that class I but not class II HDACs are involved in the downregulation of the *ATP1B1* gene expression and promoter activity by TGF-β. Further investigations elucidated a specific role for the class I HDAC member, HDAC2, in the *ATP1B1* gene repression. As HDAC2 has been detected in the alveolar epithelium, the TGF-β/HDAC2 axis could perhaps facilitate repression of the *ATP1B1* gene *in vivo* (Yin *et al*., 2006). Additionally, the importance of HDAC2 in the context of lung disease has already been stressed in pathogenesis of COPD (Barnes, 2009). The mechanism of HDAC-dependent gene repression involves the deacetylation of the histone proteins associated with the gene promoter region. The activity of the *ATP1B1* promoter was preserved in cells co-treated with TSA and TGF-β, implying that the repressive histone deacetylation occurs within the -3075 to -1238 bp region upstream from the transcriptional start site. Results of the ChIP experiments demonstrated that HDAC2 interacts with the region located between -1339 to -1241 bp upstream from the transcriptional start site of the *ATP1B1* gene. While the apparent HDAC2 abundance on the promoter was not increased after TGF-β treatment, TGF-β induced HDAC2 phosphorylation at serine 394. The HDAC2 has been found to be regulated by phosphorylation at serine 394 which potentates enzymatic activity and is an essential step during the formation of repressor complexes (Tsai and Seto, 2002). These results indicate that TGF-β executes *ATP1B1* gene repression by inducing HDAC2 activity rather than promoting sequestration of additional HDAC2 molecules to the promoter region.

In the present study, SMAD2, SMAD4, E2F5, SNAI1 and HDAC2 were reported to mediate repression of the *ATP1B1* gene in response to TGF-β. While direct interaction between HDAC2 and SMAD2, SMAD4 or E2F5 has not previously been reported, SNAI1 has been demonstrated to directly interact with HDAC2 on the *E-CADHERIN* promoter (Peinado *et al*., 2004). As mentioned above, SNAI1 was reported to repress the *ATP1B1* gene, and the TGF-β-induced interaction between SNAI1 and SMADs has been documented (Vincent *et al*., 2009, Espineda *et al*., 2004). Based on this evidence, it is reasonable to hypothesize that SMAD2, SMAD4 and SNAI1 together with HDAC2 mediate the repression of the *ATP1B1* gene expression by the TGF-β.

5.3. The inhibition of histone deacetylases rescues *Atp1b1* gene expression and reduces pulmonary edema

The availability of the ATP1B subunits is a rate limiting factor for Na,K-ATPase assembly and activity, since ATP1A subunits alone are unable to integrate into the cell membrane (Geering, 2008, Barquin *et al.*, 1997). Taking into account the fundamental role of ATP1B1 in the regulation of Na,K-ATPase, one can hypothesize that downregulation of *ATP1B1* gene expression in ARDS, and in the bleomycin model of this disease reported here, may prevent resolution of pulmonary edema by impairing Na^+ transport and AFC. The importance of the *Atp1b1* gene in the regulation of the lung water homeostasis has been confirmed in *Atp1b1* gene knock-out mice, which displayed a major reduction in the AFC (Flodby *et al*., 2012). Additionally, experiments on primary mouse alveolar epithelial cell monolayers lacking the *Atp1b1* gene demonstrated decreased transepithelial Na^+ conductance (Kim *et al*., 2011).

In vitro experiments presented in this study provide strong evidence for a key role for the HDAC2 in *ATP1B1* gene repression by TGF-β. Therefore, the possibility that HDAC inhibition would prevent *Atp1b1* gene repression in bleomycin-instilled mice has been tested. Treatment with TSA reversed downregulation of *Atp1b1* gene expression in the bleomycin model of ARDS. In parallel, animals co-treated with bleomycin and TSA displayed decreased lung wet-to-dry mass ratio. This observation signifies the presence of an inverse relationship between levels of *Atp1b1* gene expression, and levels of pulmonary edema, and indicates a beneficial effect of increased *Atp1b1* gene expression on AFC. Furthermore, the augmented expression of the *Atp1b1* gene by gene transfer has already been shown to significantly boost the Na^+ transport, AFC clearance and improve pulmonary edema (Adir *et al*., 2003, Azzam *et al*., 2002, Stern *et al*., 2000, Factor *et al*., 2000, Factor *et al*., 1998).

Collectively, these data indicate that reduced *Atp1b1* gene expression may be involved in water persistence in lungs of bleomycin-instilled mice and restored expression of the *Atp1b1* gene by TSA could augment Na,K-ATPase activity and AFC resulting in decreased edema. Moreover, the use of an HDAC inhibitor provided an alternative method to gene transfer to reactivate *Atp1b1* gene expression in order to reduce pulmonary edema. To date, HDAC inhibitors have been approved for the treatment of cutaneous T-cell lymphoma, and peripheral T-cell lymphoma and more than 80 clinical trials are currently evaluating the efficacy of over 11 different HDAC

inhibitors for the treatment of various malignancies (Ververis *et al*., 2013). Given the fact that only minor side effects were observed in these studies, it could be speculated that HDAC inhibitors could prove to be a valid pharmacological option for the treatment of ARDS.

In addition to the fundamental role in Na^+ transport and AFC, the novel function of the ATP1B1 subunit in the maintenance of tight epithelial layers has been recently proposed (Vagin *et al*., 2012). Therefore, a reduction in the level of pulmonary edema by TSA could be achieved by increased AFC and/or reduced alveolar-capillary barrier permeability. However, since TSA treatment neither reduced protein content in the BAL fluid nor decreased albumin extravasation, it can be interpreted that HDAC inhibition does not improve alveolar-capillary barrier integrity but stimulates Na^+ transport and effective AFC. This conclusion is supported by observations that *ATP1B1* gene transfer does not reduce alveolar permeability to albumin in a rat model of acute hydrostatic pulmonary edema, regardless of restored Na^+ transport and AFC (Azzam *et al*., 2002).

Despite that TSA decreased pulmonary edema, it cannot be excluded that mechanisms other than an Atp1b1-dependent increase in ion transport could restore lung water homeostasis. The possibility that TSA could improve lung water by reducing lung inflammation in the bleomycin model of ARDS was explored by characterization of the inflammatory cell profile in the alveolar space. Here, bleomycin instillation clearly provoked an inflammatory response in alveoli by increasing the fraction of the neutrophils and leukocytes, while decreasing the amount of alveolar macrophages. This dramatic change in the inflammatory cell profile by bleomycin remained unaffected by TSA treatment, implying that HDAC-mediated gene regulation does not alter the migration of inflammatory cells across the epithelial barrier. This finding is contrary to previously published results on HDAC inhibition effects in cecal ligation and puncture-induced polymicrobial sepsis and lipopolysaccharide model of ARDS. In these mice pre-treated with TSA or sodium butyrate HDAC inhibitors, neutrophil infiltration was reduced (Ni *et al*., 2010, Zhang *et al*., 2010). This discrepancy could be explained by the fact that Ni *et al.* and Zhang *et al.* used HDAC inhibitors as a preventive strategy before induction of lung injury, while in the present study, TSA was used 24 h after bleomycin instillation. Therefore, one could speculate that HDAC inhibition employed as a therapeutic approach has a limited effect on modulation of the inflammatory response. Finally, since HDAC inhibition neither altered inflammatory responses nor decreased protein levels in BAL fluid, improvement of pulmonary edema by TSA in the

bleomycin model of ARDS could be attributed to the increased AFC. The proposed mechanism of *ATP1B1* gene repression by the TGF-β/HDAC2 axis in the context of AFC and ARDS has been summarized in Figure 21.

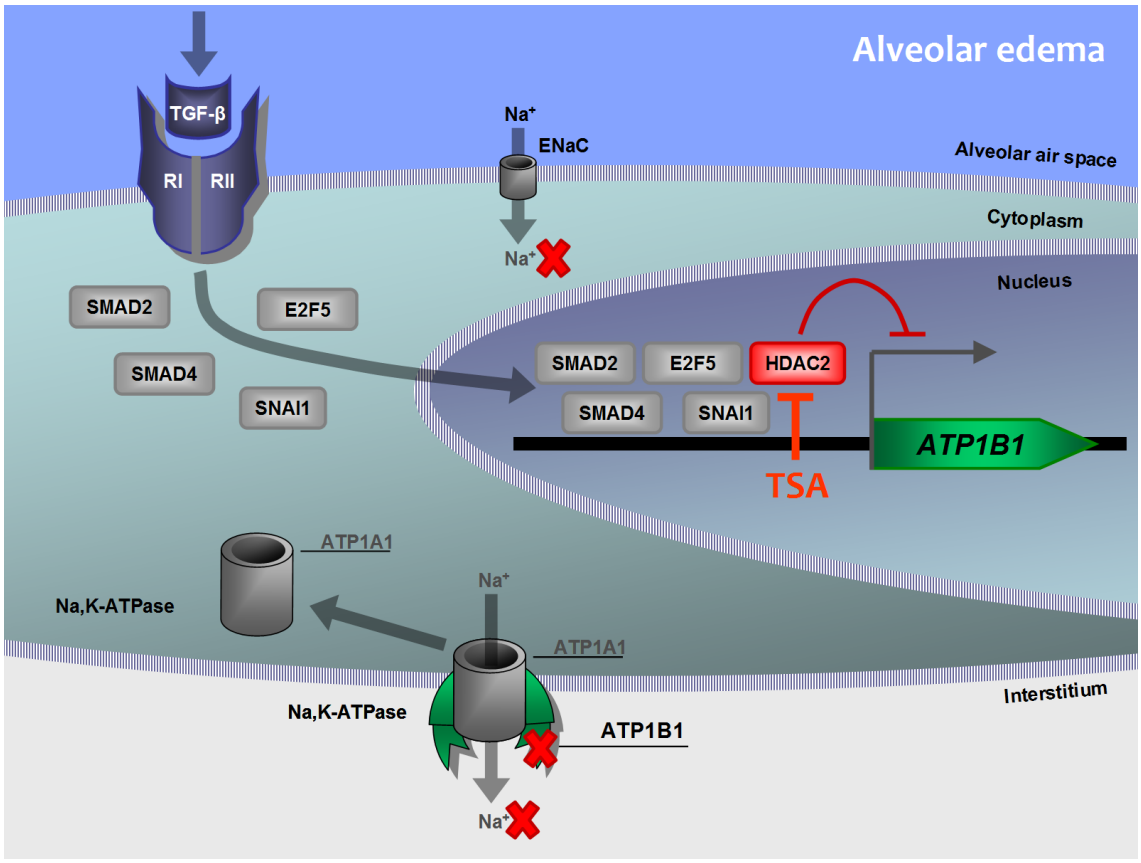

Figure 21. Model of TGF-β/HDAC2-regulated *ATP1B1* gene repression, decreased Na^+ transport and impaired alveolar fluid clearance in acute respiratory distress syndrome. Lung water balance is achieved by transepithelial Na^+ transport mediated by ENaC and Na,K-ATPase. In acute respiratory distress syndrome, activation of TGF-β signaling causes repression of the *ATP1B1* gene which is critically mediated by the epigenetic co-repressor HDAC2. Downregulation of the ATP1B1 subunit-encoding gene expression results in the decreased abundance of the Na,K-ATPase on the basolateral cell membrane and blocked Na^+ transport. Consequently, reduced Na^+ transport impairs alveolar fluid clearance (AFC) and promotes persistence of pulmonary edema. The inhibition of histone deacetylases by trichostatin A (TSA) rescues the *ATP1B1* gene expression and allows the reinsertion of the Na,K-ATPase into cell membrane. This reactivates Na^+ transport and potentates AFC which ultimately reduces pulmonary edema.

In summary, data presented here advocate a key role for the TGF-β/HDAC2 axis in repression of the *ATP1B1* gene in the alveolar epithelium in ARDS. TGF-β, a potent mediator of ARDS, activates HDAC2 which represses the *ATP1B1* gene by direct

interaction with the promoter region. This HDAC2-mediated repression mechanism was sensitive to inhibition of histone deacetylation, which resulted in induction of *ATP1B1* gene expression. Finally, HDAC inhibition also abrogated repression of the *Atp1b1* gene in bleomycin model of ARDS and decreased lung water content in parallel. As the *Atp1b1* gene performs essential role in efficient Na^+ transport and AFC, it is tempting to conclude that HDAC inhibition and subsequent increase in the *Atp1b1* gene expression reduced pulmonary edema in bleomycin model of ARDS. Ultimately, data collected in the present study indicate that inhibition of HDACs in ARDS could be a viable therapeutic option to improve pulmonary edema in this currently incurable disorder.

V. Summary

Acute respiratory distress syndrome (ARDS) is a devastating disease characterized by high mortality with no available pharmacological therapy. Transforming growth factor (TGF)-β mediates ARDS by promoting formation and persistence of alveolar edema. The deregulation of the Na,K-ATPase, a key Na^+ transporter in the alveolar epithelium, has been reported in ARDS, where impaired Na,K-ATPase function perturbs alveolar fluid clearance (AFC). In the present study, downregulation of *ATP1B1*, a gene encoding an essential subunit of the Na,K-ATPase, has been observed in ARDS patients, bleomycin model of ARDS and in TGF-β-treated primary mouse alveolar epithelial type II cells and A549 cells. A mechanism of TGF-β-regulated repression of the *ATP1B1* gene relied on SMAD2, SMAD4, SNAI1 and E2F5 transcription factors. Moreover, epigenetic machinery involving DNA methylation and action of histone deacetylases (HDAC) have been found to mediate the TGF-β-controlled downregulation of the *ATP1B1* gene. The class I HDAC member, HDAC2, has been identified as a critical element involved in *ATP1B1* gene repression, and has been observed to bind the *ATP1B1* promoter and to be activated by TGF-β signaling. The treatment with the histone deacetylase inhibitor trichostatin A (TSA) rescued expression of the *Atp1b1* gene in the bleomycin model of ARDS which was accompanied by decreased lung wet-to-dry ratio. However, TSA neither decreased alveolar-capillary barrier permeability nor alleviated inflammatory responses indicating that reduction of edema was attributable to restored Na^+ transport and increased AFC.

These data describe a novel system of HDAC-regulated repression of the *Atp1b1* gene by TGF-β which could be targeted and disrupted by HDAC inhibition in the bleomycin model of ARDS. Therefore, this study provides strong evidence to support the use of HDAC inhibitors in pharmacological therapy of ARDS.

VI. Zusammenfassung

Das akute Atemnotsyndrom (engl. *acute respiratory distress syndrome,* ARDS) ist eine verheerende Krankheit, die mit einer hohen Sterblichkeit verbunden ist und für die es keine pharmakologische Therapie gibt. Der transformierende Wachstumsfaktor (engl. *transforming growth factor* (TGF))-β fördert in ARDS die Formierung sowie den Erhalt des Alveolarödems. Wissenschaftliche Arbeiten zeigen auf, dass die Na,K-ATPase, eine der wichtigsten Na^+ Transporter im Alveolarepithel, in ARDS dereguliert ist und das eine gestörte Funktion der Na,K-ATPase zu einer verringerten alveolären Flüssigkeitsklärung (engl. *alveolar fluid clearance*, AFC) führt. In der vorliegenden Studie konnte festgestellt werden, dass es zu einer Herunterregulierung von *ATP1B1*, dem Gen, das die essentielle Untereinheit der Na,K-ATPase codiert, in Patienten mit ARDS, im Bleomycin Modell von ARDS, in TGF-β behandelten primären alveolaren Epithelzellen von Typ II der Maus und in A549 Zellen, kam. Der Mechanismus durch den TGF-β die Repression des *ATP1B1* Gens regulierte, beruhte auf den Transkriptionsfaktoren SMAD2, SMAD4, SNAI1 und E2F5. Des Weiteren konnte festgestellt werden, dass epigenetische Mechanismen, einschließlich DNA Methylierung sowie Einwirkungen der Histondeacetylasen (HDAC) an der TGF-β kontrollierten Herrunteregulierung von *ATP1B1* beteiligt sind. Das Klasse I HDAC Mitglied HDAC2, wurde als Schlüsselelement in der *ATP1B1* Genreprimierung identifiziert und es konnte gezeigt werden, dass HDAC2 den Promotor von *ATP1B1* binden und durch TGF-β aktiviert werden kann. Die Behandlung mit dem Histondeacetylaseninhibitor Trichostatin A (TSA) führte zu einer „Rettung" der *Atp1b1* Genexpression im Bleomycin Modell von ARDS und war mit einem reduzierten Nass-Trocken-Verhältnis der Lunge verbunden. Dabei führte TSA jedoch weder zu einer Reduzierung der alveolarkapillären Permeabilität noch kam es zu einer Linderung der Entzündungsreaktion, was darauf hinwies, dass das reduzierte Ödem auf die Wiederherstellung Na^+ Transports und auf eine Erhöhung des AFC zurückzuführen war.

Diese Daten beschreiben ein neues System einer HDAC-regulierten Reprimierung des *Atp1b1* Gens durch TGF-β, welches durch eine HDAC Inhibierung im Bleomycin Modell von ARDS gezielt angegriffen und umgekehrt werden kann. Daher liefert diese Studie einen starken Beweis der einen Einsatz von HDAC Inhibitoren in der pharmakologischen Therapie von ARDS rechtfertigen würde.

VII. Literature

Adir, Y., P. Factor, V. Dumasius, K. M. Ridge & J. I. Sznajder (2003) Na,K-ATPase gene transfer increases liquid clearance during ventilation-induced lung injury. *Am J Respir Crit Care Med,* 168**,** 1445-8.

Akiyoshi, S., H. Inoue, J. Hanai, K. Kusanagi, N. Nemoto, K. Miyazono & M. Kawabata (1999) c-Ski acts as a transcriptional co-repressor in transforming growth factor-beta signaling through interaction with smads. *J Biol Chem,* 274**,** 35269-77.

Alliston, T., L. Choy, P. Ducy, G. Karsenty & R. Derynck (2001) TGF-beta-induced repression of CBFA1 by Smad3 decreases cbfa1 and osteocalcin expression and inhibits osteoblast differentiation. *EMBO J,* 20**,** 2254-72.

Alliston, T., T. C. Ko, Y. Cao, Y. Y. Liang, X. H. Feng, C. Chang & R. Derynck (2005) Repression of bone morphogenetic protein and activin-inducible transcription by Evi-1. *J Biol Chem,* 280**,** 24227-37.

ARDS Network (2000) Ventilation with lower tidal volumes as compared with traditional tidal volumes for acute lung injury and the acute respiratory distress syndrome. The Acute Respiratory Distress Syndrome Network. *N Engl J Med,* 342**,** 1301-8.

ARDS Network (2011) Randomized, placebo-controlled clinical trial of an aerosolized beta(2)-agonist for treatment of acute lung injury. *Am J Respir Crit Care Med,* 184**,** 561-8.

Azzam, Z. S., V. Dumasius, F. J. Saldias, Y. Adir, J. I. Sznajder & P. Factor (2002) Na,K-ATPase overexpression improves alveolar fluid clearance in a rat model of elevated left atrial pressure. *Circulation,* 105**,** 497-501.

Baba, Y., T. Yazawa, Y. Kanegae, S. Sakamoto, I. Saito, N. Morimura, T. Goto, Y. Yamada & K. Kurahashi (2007) Keratinocyte growth factor gene transduction ameliorates acute lung injury and mortality in mice. *Hum Gene Ther,* 18**,** 130-41.

Barnes, P. J. (2009) Histone deacetylase-2 and airway disease. *Ther Adv Respir Dis,* 3**,** 235-43.

Barquin, N., D. E. Ciccolella, K. M. Ridge & J. I. Sznajder (1997) Dexamethasone upregulates the Na-K-ATPase in rat alveolar epithelial cells. *Am J Physiol,* 273**,** L825-30.

Berger, G., J. Guetta, G. Klorin, R. Badarneh, E. Braun, V. Brod, N. A. Saleh, A. Katz, H. Bitterman & Z. S. Azzam (2011) Sepsis impairs alveolar epithelial function by downregulating Na-K-ATPase pump. *Am J Physiol Lung Cell Mol Physiol,* 301**,** L23-30.

Bernard, G. R., A. Artigas, K. L. Brigham, J. Carlet, K. Falke, L. Hudson, M. Lamy, J. R. LeGall, A. Morris & R. Spragg (1994) Report of the American-European Consensus conference on acute respiratory distress syndrome: definitions, mechanisms, relevant outcomes, and clinical trial coordination. Consensus Committee. *J Crit Care,* 9**,** 72-81.

Berthiaume, Y. & M. A. Matthay (2007) Alveolar edema fluid clearance and acute lung injury. *Respir Physiol Neurobiol,* 159**,** 350-9.

Bieliauskas, A. V. & M. K. Pflum (2008) Isoform-selective histone deacetylase inhibitors. *Chem Soc Rev,* 37**,** 1402-13.

Blokzijl, A., C. Dahlqvist, E. Reissmann, A. Falk, A. Moliner, U. Lendahl & C. F. Ibanez (2003) Cross-talk between the Notch and TGF-beta signaling pathways

mediated by interaction of the Notch intracellular domain with Smad3. *J Cell Biol,* 163**,** 723-8.

Bone, R. C., P. B. Francis & A. K. Pierce (1976) Intravascular coagulation associated with the adult respiratory distress syndrome. *Am J Med,* 61**,** 585-9.

Borok, Z., S. I. Danto, L. L. Dimen, X. L. Zhang & R. L. Lubman (1998) Na(+)-K(+)-ATPase expression in alveolar epithelial cells: upregulation of active ion transport by KGF. *Am J Physiol,* 274**,** L149-58.

Budinger, G. R., N. S. Chandel, H. K. Donnelly, J. Eisenbart, M. Oberoi & M. Jain (2005) Active transforming growth factor-beta1 activates the procollagen I promoter in patients with acute lung injury. *Intensive Care Med,* 31**,** 121-8.

Chen, C. R., Y. Kang, P. M. Siegel & J. Massague (2002) E2F4/5 and p107 as Smad cofactors linking the TGFbeta receptor to c-myc repression. *Cell,* 110**,** 19-32.

Cordenonsi, M., S. Dupont, S. Maretto, A. Insinga, C. Imbriano & S. Piccolo (2003) Links between tumor suppressors: p53 is required for TGF-beta gene responses by cooperating with Smads. *Cell,* 113**,** 301-14.

Corti, M., A. R. Brody & J. H. Harrison (1996) Isolation and primary culture of murine alveolar type II cells. *Am J Respir Cell Mol Biol,* 14**,** 309-15.

Dhainaut, J. F., J. Charpentier & J. D. Chiche (2003) Transforming growth factor-beta: a mediator of cell regulation in acute respiratory distress syndrome. *Crit Care Med,* 31**,** S258-64.

Dobbs, L. G., R. Gonzalez, M. A. Matthay, E. P. Carter, L. Allen & A. S. Verkman (1998) Highly water-permeable type I alveolar epithelial cells confer high water permeability between the airspace and vasculature in rat lung. *Proc Natl Acad Sci U S A,* 95**,** 2991-6.

Egli, M., H. Duplain, M. Lepori, S. Cook, P. Nicod, E. Hummler, C. Sartori & U. Scherrer (2004) Defective respiratory amiloride-sensitive sodium transport predisposes to pulmonary oedema and delays its resolution in mice. *J Physiol,* 560**,** 857-65.

Eickelberg, O. & R. E. Morty (2007) Transforming growth factor beta/bone morphogenic protein signaling in pulmonary arterial hypertension: remodeling revisited. *Trends Cardiovasc Med,* 17**,** 263-9.

Eisner, M. D., T. Thompson, L. D. Hudson, J. M. Luce, D. Hayden, D. Schoenfeld, M. A. Matthay & N. Acute Respiratory Distress Syndrome (2001) Efficacy of low tidal volume ventilation in patients with different clinical risk factors for acute lung injury and the acute respiratory distress syndrome. *Am J Respir Crit Care Med,* 164**,** 231-6.

Espineda, C. E., J. H. Chang, J. Twiss, S. A. Rajasekaran & A. K. Rajasekaran (2004) Repression of Na,K-ATPase beta1-subunit by the transcription factor snail in carcinoma. *Mol Biol Cell,* 15**,** 1364-73.

Evans, D. J., P. S. Matsumoto, J. H. Widdicombe, C. Li-Yun, A. A. Maminishkis & S. S. Miller (1998) Pseudomonas aeruginosa induces changes in fluid transport across airway surface epithelia. *Am J Physiol,* 275**,** C1284-90.

Factor, P., V. Dumasius, F. Saldias, L. A. Brown & J. I. Sznajder (2000) Adenovirus-mediated transfer of an Na+/K+-ATPase beta1 subunit gene improves alveolar fluid clearance and survival in hyperoxic rats. *Hum Gene Ther,* 11**,** 2231-42.

Factor, P., F. Saldias, K. Ridge, V. Dumasius, J. Zabner, H. A. Jaffe, G. Blanco, M. Barnard, R. Mercer, R. Perrin & J. I. Sznajder (1998) Augmentation of lung liquid clearance via adenovirus-mediated transfer of a Na,K-ATPase beta1 subunit gene. *J Clin Invest,* 102**,** 1421-30.

Fahy, R. J., F. Lichtenberger, C. B. McKeegan, G. J. Nuovo, C. B. Marsh & M. D. Wewers (2003) The acute respiratory distress syndrome: a role for transforming growth factor-beta 1. *Am J Respir Cell Mol Biol,* 28**,** 499-503.

Feng, X. H. & R. Derynck (2005) Specificity and versatility in tgf-beta signaling through Smads. *Annu Rev Cell Dev Biol,* 21**,** 659-93.

Feng, X. H., X. Lin & R. Derynck (2000) Smad2, Smad3 and Smad4 cooperate with Sp1 to induce p15(Ink4B) transcription in response to TGF-beta. *EMBO J,* 19**,** 5178-93.

Feng, X. H., Y. Zhang, R. Y. Wu & R. Derynck (1998) The tumor suppressor Smad4/DPC4 and transcriptional adaptor CBP/p300 are coactivators for smad3 in TGF-beta-induced transcriptional activation. *Genes Dev,* 12**,** 2153-63.

Flodby, P., Z. Borok, D. Gao, Y. Kim, K. Kim & E. D. Crandall (2012) Role of sodium pump β1 subunit in adult mouse lung alveolar fluid homeostasis. *FASEB J,* 26, 1069.6.

Folkesson, H. G., J. F. Pittet, G. Nitenberg & M. A. Matthay (1996) Transforming growth factor-alpha increases alveolar liquid clearance in anesthetized ventilated rats. *Am J Physiol,* 271**,** L236-44.

Force, A. D. T., V. M. Ranieri, G. D. Rubenfeld, B. T. Thompson, N. D. Ferguson, E. Caldwell, E. Fan, L. Camporota & A. S. Slutsky (2012) Acute respiratory distress syndrome: the Berlin Definition. *JAMA,* 307**,** 2526-33.

Fragiadaki, M., T. Ikeda, A. Witherden, R. M. Mason, D. Abraham & G. Bou-Gharios (2011) High doses of TGF-beta potently suppress type I collagen via the transcription factor CUX1. *Mol Biol Cell,* 22**,** 1836-44.

Frank, J., J. Roux, H. Kawakatsu, G. Su, A. Dagenais, Y. Berthiaume, M. Howard, C. M. Canessa, X. Fang, D. Sheppard, M. A. Matthay & J. F. Pittet (2003) Transforming growth factor-beta1 decreases expression of the epithelial sodium channel alphaENaC and alveolar epithelial vectorial sodium and fluid transport via an ERK1/2-dependent mechanism. *J Biol Chem,* 278**,** 43939-50.

Gao Smith, F., G. D. Perkins, S. Gates, D. Young, D. F. McAuley, W. Tunnicliffe, Z. Khan, S. E. Lamb & B.-s. investigators (2012) Effect of intravenous beta-2 agonist treatment on clinical outcomes in acute respiratory distress syndrome (BALTI-2): a multicentre, randomised controlled trial. *Lancet,* 379**,** 229-35.

Geering, K. (2006) FXYD proteins: new regulators of Na-K-ATPase. *Am J Physiol Renal Physiol,* 290**,** F241-50.

Geering, K. (2008) Functional roles of Na,K-ATPase subunits. *Curr Opin Nephrol Hypertens,* 17**,** 526-32.

Geiser, T. (2003) Mechanisms of alveolar epithelial repair in acute lung injury-a translational approach. *Swiss Med Wkly,* 133**,** 586-90.

Ghosh, A. K., W. Yuan, Y. Mori & J. Varga (2000) Smad-dependent stimulation of type I collagen gene expression in human skin fibroblasts by TGF-beta involves functional cooperation with p300/CBP transcriptional coactivators. *Oncogene,* 19**,** 3546-55.

Goumans, M. J. & C. Mummery (2000) Functional analysis of the TGFbeta receptor/Smad pathway through gene ablation in mice. *Int J Dev Biol,* 44**,** 253-65.

Guidot, D. M., H. G. Folkesson, L. Jain, J. I. Sznajder, J. F. Pittet & M. A. Matthay (2006) Integrating acute lung injury and regulation of alveolar fluid clearance. *Am J Physiol Lung Cell Mol Physiol,* 291**,** L301-6.

Hardie, W. D., D. R. Prows, A. Piljan-Gentle, M. R. Dunlavy, S. C. Wesselkamper, G. D. Leikauf & T. R. Korfhagen (2002) Dose-related protection from

nickel-induced lung injury in transgenic mice expressing human transforming growth factor-alpha. *Am J Respir Cell Mol Biol,* 26**,** 430-7.

Hooper, M. & G. Bernard (2011) Pharmacogenetic treatment of acute respiratory distress syndrome. *Minerva Anestesiol,* 77**,** 624-36.

Hua, X., Z. A. Miller, G. Wu, Y. Shi & H. F. Lodish (1999) Specificity in transforming growth factor beta-induced transcription of the plasminogen activator inhibitor-1 gene: interactions of promoter DNA, transcription factor muE3, and Smad proteins. *Proc Natl Acad Sci U S A,* 96**,** 13130-5.

Huang, F. & Y. G. Chen (2012) Regulation of TGF-beta receptor activity. *Cell Biosci,* 2**,** 9.

Hurst, V. I., P. L. Goldberg, F. L. Minnear, R. L. Heimark & P. A. Vincent (1999) Rearrangement of adherens junctions by transforming growth factor-beta1: role of contraction. *Am J Physiol,* 276**,** L582-95.

Itoh, S., J. Ericsson, J. Nishikawa, C. H. Heldin & P. ten Dijke (2000) The transcriptional co-activator P/CAF potentiates TGF-beta/Smad signaling. *Nucleic Acids Res,* 28**,** 4291-8.

Kahata, K., M. Hayashi, M. Asaka, U. Hellman, H. Kitagawa, J. Yanagisawa, S. Kato, T. Imamura & K. Miyazono (2004) Regulation of transforming growth factor-beta and bone morphogenetic protein signalling by transcriptional coactivator GCN5. *Genes Cells,* 9**,** 143-51.

Kang, J. S., T. Alliston, R. Delston & R. Derynck (2005) Repression of Runx2 function by TGF-beta through recruitment of class II histone deacetylases by Smad3. *EMBO J,* 24**,** 2543-55.

Kang, Y., C. R. Chen & J. Massague (2003) A self-enabling TGFbeta response coupled to stress signaling: Smad engages stress response factor ATF3 for Id1 repression in epithelial cells. *Mol Cell,* 11**,** 915-26.

Kato, Y., R. Habas, Y. Katsuyama, A. M. Naar & X. He (2002) A component of the ARC/Mediator complex required for TGF beta/Nodal signalling. *Nature,* 418**,** 641-6.

Keating, D. T., D. M. Sadlier, A. Patricelli, S. M. Smith, D. Walls, J. J. Egan & P. P. Doran (2006) Microarray identifies ADAM family members as key responders to TGF-beta1 in alveolar epithelial cells. *Respir Res,* 7**,** 114.

Khalil, N., R. N. O'Connor, K. C. Flanders & H. Unruh (1996) TGF-beta 1, but not TGF-beta 2 or TGF-beta 3, is differentially present in epithelial cells of advanced pulmonary fibrosis: an immunohistochemical study. *Am J Respir Cell Mol Biol,* 14**,** 131-8.

Kim, J., K. Johnson, H. J. Chen, S. Carroll & A. Laughon (1997) Drosophila Mad binds to DNA and directly mediates activation of vestigial by Decapentaplegic. *Nature,* 388**,** 304-8.

Kurisaki, K., A. Kurisaki, U. Valcourt, A. A. Terentiev, K. Pardali, P. Ten Dijke, C. H. Heldin, J. Ericsson & A. Moustakas (2003) Nuclear factor YY1 inhibits transforming growth factor beta- and bone morphogenetic protein-induced cell differentiation. *Mol Cell Biol,* 23**,** 4494-510.

Laffon, M., J. F. Pittet, K. Modelska, M. A. Matthay & D. M. Young (1999) Interleukin-8 mediates injury from smoke inhalation to both the lung endothelial and the alveolar epithelial barriers in rabbits. *Am J Respir Crit Care Med,* 160**,** 1443-9.

Lecuona, E., F. Saldias, A. Comellas, K. Ridge, C. Guerrero & J. I. Sznajder (1999) Ventilator-associated lung injury decreases lung ability to clear edema in rats. *Am J Respir Crit Care Med,* 159**,** 603-9.

Lecuona, E., H. E. Trejo & J. I. Sznajder (2007) Regulation of Na,K-ATPase during acute lung injury. *J Bioenerg Biomembr,* 39**,** 391-5.

Liberati, N. T., M. Moniwa, A. J. Borton, J. R. Davie & X. F. Wang (2001) An essential role for Mad homology domain 1 in the association of Smad3 with histone deacetylase activity*. *J Biol Chem,* 276**,** 22595-603.

Lipes, J., A. Bojmehrani & F. Lellouche (2012) Low Tidal Volume Ventilation in Patients without Acute Respiratory Distress Syndrome: A Paradigm Shift in Mechanical Ventilation. *Crit Care Res Pract,* 2012**,** 416862.

Looney, M. R., J. X. Nguyen, Y. Hu, J. A. Van Ziffle, C. A. Lowell & M. A. Matthay (2009) Platelet depletion and aspirin treatment protect mice in a two-event model of transfusion-related acute lung injury. *J Clin Invest,* 119**,** 3450-61.

Looney, M. R., X. Su, J. A. Van Ziffle, C. A. Lowell & M. A. Matthay (2006) Neutrophils and their Fc gamma receptors are essential in a mouse model of transfusion-related acute lung injury. *J Clin Invest,* 116**,** 1615-23.

Lopez-Rovira, T., E. Chalaux, J. L. Rosa, R. Bartrons & F. Ventura (2000) Interaction and functional cooperation of NF-kappa B with Smads. Transcriptional regulation of the junB promoter. *J Biol Chem,* 275**,** 28937-46.

Ma, T., N. Fukuda, Y. Song, M. A. Matthay & A. S. Verkman (2000) Lung fluid transport in aquaporin-5 knockout mice. *J Clin Invest,* 105**,** 93-100.

Marshall, R., G. Bellingan & G. Laurent (1998) The acute respiratory distress syndrome: fibrosis in the fast lane. *Thorax,* 53**,** 815-7.

Massague, J. & Y. G. Chen (2000) Controlling TGF-beta signaling. *Genes Dev,* 14**,** 627-44.

Massague, J. & R. R. Gomis (2006) The logic of TGFbeta signaling. *FEBS Lett,* 580**,** 2811-20.

Massague, J., J. Seoane & D. Wotton (2005) Smad transcription factors. *Genes Dev,* 19**,** 2783-810.

Matthay, M. A., H. G. Folkesson & C. Clerici (2002) Lung epithelial fluid transport and the resolution of pulmonary edema. *Physiol Rev,* 82**,** 569-600.

Matthay, M. A. & J. P. Wiener-Kronish (1990) Intact epithelial barrier function is critical for the resolution of alveolar edema in humans. *Am Rev Respir Dis,* 142**,** 1250-7.

Matthay, M. A. & R. L. Zemans (2011) The acute respiratory distress syndrome: pathogenesis and treatment. *Annu Rev Pathol,* 6**,** 147-63.

Matthay, M. A. & G. A. Zimmerman (2005) Acute lung injury and the acute respiratory distress syndrome: four decades of inquiry into pathogenesis and rational management. *Am J Respir Cell Mol Biol,* 33**,** 319-27.

Modelska, K., J. F. Pittet, H. G. Folkesson, V. Courtney Broaddus & M. A. Matthay (1999) Acid-induced lung injury. Protective effect of anti-interleukin-8 pretreatment on alveolar epithelial barrier function in rabbits. *Am J Respir Crit Care Med,* 160**,** 1450-6.

Moloney, E. D. & T. W. Evans (2003) Pathophysiology and pharmacological treatment of pulmonary hypertension in acute respiratory distress syndrome. *Eur Respir J,* 21**,** 720-7.

Morth, J. P., B. P. Pedersen, M. S. Toustrup-Jensen, T. L. Sorensen, J. Petersen, J. P. Andersen, B. Vilsen & P. Nissen (2007) Crystal structure of the sodium-potassium pump. *Nature,* 450**,** 1043-9.

Morty, R. E., O. Eickelberg & W. Seeger (2007) Alveolar fluid clearance in acute lung injury: what have we learned from animal models and clinical studies? *Intensive Care Med,* 33**,** 1229-40.

Munger, J. S. & D. Sheppard (2011) Cross talk among TGF-beta signaling pathways, integrins, and the extracellular matrix. *Cold Spring Harb Perspect Biol,* 3**,** a005017.

Ni, Y. F., J. Wang, X. L. Yan, F. Tian, J. B. Zhao, Y. J. Wang & T. Jiang (2010) Histone deacetylase inhibitor, butyrate, attenuates lipopolysaccharide-induced acute lung injury in mice. *Respir Res,* 11**,** 33.

Nishihara, A., J. I. Hanai, N. Okamoto, J. Yanagisawa, S. Kato, K. Miyazono & M. Kawabata (1998) Role of p300, a transcriptional coactivator, in signalling of TGF-beta. *Genes Cells,* 3**,** 613-23.

Peinado, H., E. Ballestar, M. Esteller & A. Cano (2004) Snail mediates E-cadherin repression by the recruitment of the Sin3A/histone deacetylase 1 (HDAC1)/HDAC2 complex. *Mol Cell Biol,* 24**,** 306-19.

Perkins, G. D., D. F. McAuley, D. R. Thickett & F. Gao (2006) The beta-agonist lung injury trial (BALTI): a randomized placebo-controlled clinical trial. *Am J Respir Crit Care Med,* 173**,** 281-7.

Pitchford, S. C., H. Yano, R. Lever, Y. Riffo-Vasquez, S. Ciferri, M. J. Rose, S. Giannini, S. Momi, D. Spina, B. O'Connor, P. Gresele & C. P. Page (2003) Platelets are essential for leukocyte recruitment in allergic inflammation. *J Allergy Clin Immunol,* 112**,** 109-18.

Pittet, J. F., M. J. Griffiths, T. Geiser, N. Kaminski, S. L. Dalton, X. Huang, L. A. Brown, P. J. Gotwals, V. E. Koteliansky, M. A. Matthay & D. Sheppard (2001) TGF-beta is a critical mediator of acute lung injury. *J Clin Invest,* 107**,** 1537-44.

Pouponnot, C., L. Jayaraman & J. Massague (1998) Physical and functional interaction of SMADs and p300/CBP. *J Biol Chem,* 273**,** 22865-8.

Ranganathan, P., A. Agrawal, R. Bhushan, A. K. Chavalmane, R. K. Kalathur, T. Takahashi & P. Kondaiah (2007) Expression profiling of genes regulated by TGF-beta: differential regulation in normal and tumour cells. *BMC Genomics,* 8**,** 98.

Ross, S., E. Cheung, T. G. Petrakis, M. Howell, W. L. Kraus & C. S. Hill (2006) Smads orchestrate specific histone modifications and chromatin remodeling to activate transcription. *EMBO J,* 25**,** 4490-502.

Ross, S. & C. S. Hill (2008) How the Smads regulate transcription. *Int J Biochem Cell Biol,* 40**,** 383-408.

Rubenfeld, G. D., E. Caldwell, E. Peabody, J. Weaver, D. P. Martin, M. Neff, E. J. Stern & L. D. Hudson (2005) Incidence and outcomes of acute lung injury. *N Engl J Med,* 353**,** 1685-93.

Santibanez, J. F., M. Quintanilla & C. Bernabeu (2011) TGF-beta/TGF-beta receptor system and its role in physiological and pathological conditions. *Clin Sci (Lond),* 121**,** 233-51.

Sartori, C. & M. A. Matthay (2002) Alveolar epithelial fluid transport in acute lung injury: new insights. *Eur Respir J,* 20**,** 1299-313.

Seoane, J., H. V. Le, L. Shen, S. A. Anderson & J. Massague (2004) Integration of Smad and forkhead pathways in the control of neuroepithelial and glioblastoma cell proliferation. *Cell,* 117**,** 211-23.

Shen, X., P. P. Hu, N. T. Liberati, M. B. Datto, J. P. Frederick & X. F. Wang (1998) TGF-beta-induced phosphorylation of Smad3 regulates its interaction with coactivator p300/CREB-binding protein. *Mol Biol Cell,* 9**,** 3309-19.

Sheppard, D. (2006) Transforming growth factor beta: a central modulator of pulmonary and airway inflammation and fibrosis. *Proc Am Thorac Soc,* 3**,** 413-7.

Shi, Y., Y. F. Wang, L. Jayaraman, H. Yang, J. Massague & N. P. Pavletich (1998) Crystal structure of a Smad MH1 domain bound to DNA: insights on DNA binding in TGF-beta signaling. *Cell,* 94**,** 585-94.

Sime, P. J., Z. Xing, F. L. Graham, K. G. Csaky & J. Gauldie (1997) Adenovector-mediated gene transfer of active transforming growth factor-beta1 induces prolonged severe fibrosis in rat lung. *J Clin Invest,* 100**,** 768-76.

Stern, M., K. Ulrich, C. Robinson, J. Copeland, U. Griesenbach, C. Masse, S. Cheng, F. Munkonge, D. Geddes, Y. Berthiaume & E. Alton (2000) Pretreatment with cationic lipid-mediated transfer of the Na+K+-ATPase pump in a mouse model in vivo augments resolution of high permeability pulmonary oedema. *Gene Ther,* 7**,** 960-6.

Stroschein, S. L., W. Wang, S. Zhou, Q. Zhou & K. Luo (1999) Negative feedback regulation of TGF-beta signaling by the SnoN oncoprotein. *Science,* 286**,** 771-4.

ten Dijke, P. & C. S. Hill (2004) New insights into TGF-beta-Smad signalling. *Trends Biochem Sci,* 29**,** 265-73.

Thillainadesan, G., J. M. Chitilian, M. Isovic, J. N. Ablack, J. S. Mymryk, M. Tini & J. Torchia (2012) TGF-beta-dependent active demethylation and expression of the p15ink4b tumor suppressor are impaired by the ZNF217/CoREST complex. *Mol Cell,* 46**,** 636-49.

Tomashefski, J. F., Jr. (2000) Pulmonary pathology of acute respiratory distress syndrome. *Clin Chest Med,* 21**,** 435-66.

Tomashefski, J. F., Jr., P. Davies, C. Boggis, R. Greene, W. M. Zapol & L. M. Reid (1983) The pulmonary vascular lesions of the adult respiratory distress syndrome. *Am J Pathol,* 112**,** 112-26.

Tsai, S. C. & E. Seto (2002) Regulation of histone deacetylase 2 by protein kinase CK2. *J Biol Chem,* 277**,** 31826-33.

Vadasz, I., R. E. Morty, A. Olschewski, M. Konigshoff, M. G. Kohstall, H. A. Ghofrani, F. Grimminger & W. Seeger (2005) Thrombin impairs alveolar fluid clearance by promoting endocytosis of Na+,K+-ATPase. *Am J Respir Cell Mol Biol,* 33**,** 343-54.

Vagin, O., L. A. Dada, E. Tokhtaeva & G. Sachs (2012) The Na-K-ATPase alpha(1)beta(1) heterodimer as a cell adhesion molecule in epithelia. *Am J Physiol Cell Physiol,* 302**,** C1271-81.

Ververis, K., A. Hiong, T. C. Karagiannis & P. V. Licciardi (2013) Histone deacetylase inhibitors (HDACIs): multitargeted anticancer agents. *Biologics,* 7**,** 47-60.

Vincent, T., E. P. Neve, J. R. Johnson, A. Kukalev, F. Rojo, J. Albanell, K. Pietras, I. Virtanen, L. Philipson, P. L. Leopold, R. G. Crystal, A. G. de Herreros, A. Moustakas, R. F. Pettersson & J. Fuxe (2009) A SNAIL1-SMAD3/4 transcriptional repressor complex promotes TGF-beta mediated epithelial-mesenchymal transition. *Nat Cell Biol,* 11**,** 943-50.

Ward, P. A. & G. W. Hunninghake (1998) Lung inflammation and fibrosis. *Am J Respir Crit Care Med,* 157**,** S123-9.

Ware, L. B. (2006) Pathophysiology of acute lung injury and the acute respiratory distress syndrome. *Semin Respir Crit Care Med,* 27**,** 337-49.

Ware, L. B., J. A. Golden, W. E. Finkbeiner & M. A. Matthay (1999) Alveolar epithelial fluid transport capacity in reperfusion lung injury after lung transplantation. *Am J Respir Crit Care Med,* 159**,** 980-8.

Ware, L. B. & M. A. Matthay (2000) The acute respiratory distress syndrome. *N Engl J Med,* 342**,** 1334-49.

Ware, L. B. & M. A. Matthay (2001) Alveolar fluid clearance is impaired in the majority of patients with acute lung injury and the acute respiratory distress syndrome. *Am J Respir Crit Care Med,* 163**,** 1376-83.

Wesselkamper, S. C., L. M. Case, L. N. Henning, M. T. Borchers, J. W. Tichelaar, J. M. Mason, N. Dragin, M. Medvedovic, M. A. Sartor, C. R. Tomlinson & G. D. Leikauf (2005) Gene expression changes during the development of acute lung injury: role of transforming growth factor beta. *Am J Respir Crit Care Med,* 172**,** 1399-411.

Wiener-Kronish, J. P., K. H. Albertine & M. A. Matthay (1991) Differential responses of the endothelial and epithelial barriers of the lung in sheep to Escherichia coli endotoxin. *J Clin Invest,* 88**,** 864-75.

Wilkinson, D. S., S. K. Ogden, S. A. Stratton, J. L. Piechan, T. T. Nguyen, G. A. Smulian & M. C. Barton (2005) A direct intersection between p53 and transforming growth factor beta pathways targets chromatin modification and transcription repression of the alpha-fetoprotein gene. *Mol Cell Biol,* 25**,** 1200-12.

Willis, B. C. & Z. Borok (2007) TGF-beta-induced EMT: mechanisms and implications for fibrotic lung disease. *Am J Physiol Lung Cell Mol Physiol,* 293**,** L525-34.

Willis, B. C., K. J. Kim, X. Li, J. Liebler, E. D. Crandall & Z. Borok (2003) Modulation of ion conductance and active transport by TGF-beta 1 in alveolar epithelial cell monolayers. *Am J Physiol Lung Cell Mol Physiol,* 285**,** L1192-200.

Wotton, D., R. S. Lo, S. Lee & J. Massague (1999) A Smad transcriptional corepressor. *Cell,* 97**,** 29-39.

Wu, J. & M. Grunstein (2000) 25 years after the nucleosome model: chromatin modifications. *Trends Biochem Sci,* 25**,** 619-23.

Wu, M. Y. & C. S. Hill (2009) Tgf-beta superfamily signaling in embryonic development and homeostasis. *Dev Cell,* 16**,** 329-43.

Yamasaki, M., H. R. Kang, R. J. Homer, S. P. Chapoval, S. J. Cho, B. J. Lee, J. A. Elias & C. G. Lee (2008) P21 regulates TGF-beta1-induced pulmonary responses via a TNF-alpha-signaling pathway. *Am J Respir Cell Mol Biol,* 38**,** 346-53.

Yin, Z., L. Gonzales, V. Kolla, N. Rath, Y. Zhang, M. M. Lu, S. Kimura, P. L. Ballard, M. F. Beers, J. A. Epstein & E. E. Morrisey (2006) Hop functions downstream of Nkx2.1 and GATA6 to mediate HDAC-dependent negative regulation of pulmonary gene expression. *Am J Physiol Lung Cell Mol Physiol,* 291**,** L191-9.

Zarbock, A. & K. Ley (2009) The role of platelets in acute lung injury (ALI). *Front Biosci,* 14**,** 150-8.

Zarbock, A., K. Singbartl & K. Ley (2006) Complete reversal of acid-induced acute lung injury by blocking of platelet-neutrophil aggregation. *J Clin Invest,* 116**,** 3211-9.

Zawel, L., J. L. Dai, P. Buckhaults, S. Zhou, K. W. Kinzler, B. Vogelstein & S. E. Kern (1998) Human Smad3 and Smad4 are sequence-specific transcription activators. *Mol Cell,* 1**,** 611-7.

Zhang, F., L. D. Nielsen, J. J. Lucas & R. J. Mason (2004) Transforming growth factor-beta antagonizes alveolar type II cell proliferation induced by keratinocyte growth factor. *Am J Respir Cell Mol Biol,* 31**,** 679-86.

Zhang, L., S. Jin, C. Wang, R. Jiang & J. Wan (2010) Histone deacetylase inhibitors attenuate acute lung injury during cecal ligation and puncture-induced polymicrobial sepsis. *World J Surg,* 34**,** 1676-83.

Zhao, R. Z., H. G. Nie, X. F. Su, D. Y. Han, A. Lee, Y. Huang, Y. Chang, S. Matalon & H. L. Ji (2012) Characterization of a novel splice variant of delta ENaC subunit in human lungs. *Am J Physiol Lung Cell Mol Physiol,* 302**,** L1262-72.

VIII. Acknowledgements

I would like to express my appreciation to all following ones for their kind assistance during my PhD journey.

My first gratitude goes to my supervisor Dr. Rory Morty, who gave me a chance to work in his laboratory and who accepted me in the Molecular Biology and Medicine of the Lung international graduate programme. I am sincerely thankful for his guidance and enthusiasm during my research which ultimately made this thesis possible.

I would like to thank Prof. Dr. Werner Seeger, for giving me the opportunity to be in the Molecular Biology and Medicine of the Lung international graduate programme. I also would like to thank you for making me realise how dedication and passion of a single person can lead to biggest projects.

I am sincerely grateful to Dr. Malgorzata Wygrecka for her professional advice and stimulating discussions. Thank you for your understanding, patience and for helping me in realization of this project.

Simone Becker, Anna Blume, Jordi Ruiz Camp, Alicia Madurga Hernandez, Tatyana Likhoshvay, Ivana Mizikova, Gero Niess and Elpidoforos Sakkas, I would like to thank you all AG Morty lab members for your help, advice and many, many amusing moments. Monika Haselbauer and Ursula Reinhardt, thank you ladies for your invaluable assistance with administrative issues. It has been a great pleasure working with all of you!

I would like to thank Kasia for her love and patience which gave me strength to endure moments of doubt. Eryk, my son, thank you for sleeping through the night and for all these funny little moments every day you gave me. Finally, I would like to thank my parents and sister for their priceless support and faith in me.

Der Lebenslauf wurde aus der elektronischen Version der Arbeit entfernt.

The curriculum vitae was removed from the electronic version of the paper.

X. Declaration

Hiermit erkläre ich, dass ich die vorliegende Arbeit selbständig und ohne unzulässige Hilfe oder Benutzung anderer als der angegebenen Hilfsmittel angefertigt habe. Alle Textstellen, die wörtlich oder sinngemäß aus veröffentlichten oder nichtveröffentlichten Schriften entnommen sind, und alle Angaben, die auf mündlichen Auskünften beruhen, sind als solche kenntlich gemacht. Bei den von mir durchgeführten und in der Dissertation erwähnten Untersuchungen habe ich die Grundsätze guter wissenschaftlicher Praxis, wie sie in der „Satzung der Justus-Liebig-Universität Gießen zur Sicherung guter wissenschaftlicher Praxis“ niedergelegt sind, eingehalten sowie ethische, datenschutzrechtliche und tierschutzrechtliche Grundsätze befolgt. Ich versichere, dass Dritte von mir weder unmittelbar noch mittelbar geldwerte Leistungen für Arbeiten erhalten haben, die im Zusammenhang mit dem Inhalt der vorgelegten Dissertation stehen, oder habe diese nachstehend spezifiziert. Die vorgelegte Arbeit wurde weder im Inland noch im Ausland in gleicher oder ähnlicher Form einer anderen Prüfungsbehörde zum Zweck einer Promotion oder eines anderen Prüfungsverfahrens vorgelegt. Alles aus anderen Quellen und von anderen Personen übernommene Material, das in der Arbeit verwendet wurde oder auf das direkt Bezug genommen wird, wurde als solches kenntlich gemacht. Insbesondere wurden alle Personen genannt, die direkt und indirekt an der Entstehung der vorliegenden Arbeit beteiligt waren. Mit der Überprüfung meiner Arbeit durch eine Plagiatserkennungssoftware bzw. ein internetbasiertes Softwareprogramm erkläre ich mich einverstanden.

_____ _____

Ort, Datum Unterschrift